Nuclear Physics B56 (1973) 386–439 North-Holland Publishing Company

NON-DIFFRACTIVE PRODUCTION OF MESON RESONANCES*

G.C FOX and A.J.G. HEY**
California Institute of Technology, Pasadena, California 91109

Received 15 January 1973

Abstract We study the peripheral cross sections of resonances that *cannot* be produced by π-exchange In particular, we concentrate on the four meson nonets expected as $L = 1$ quark states (i e., the $J^P = 0^+$ $\pi_N(980)$, $J^P = 1^+$ A_1, B, $J^P = 2^+$ A_2) We use SU(3), Regge poles, factorization, exchange degeneracy, pole extrapolation, and the vector-meson–photon analogy We predict the cross sections in both photoproduction and non-diffractive hadronic reactions In passing, we discuss the large unnatural-parity (B, $K-Q_B$) exchange contributions and even the possibility of studying $\pi\pi \to \pi\omega$ while avoiding the B production background

1. Introduction

In the past four years or so, meson spectroscopy has been conspicuous for the lack of decisive answers to important theoretical questions [1, 2]. For instance, the parameters and even existence of the predicted $L = 1$ quark resonance nonets are still unclear

One reason for lack of progress is our ignorance of diffraction processes. The confusing nature of diffractive meson production was recently reviewed [3, 4], and it was concluded that *peripheral non-diffractive resonance reactions* would be the most fruitful for studying resonance parameters (mass/width) and quantum numbers. In this paper, we would like to study quantitatively the theoretical predictions for these processes and also the implications of the rather sparse experimental data now available. The reader is referred to the earlier review [3] for a purely qualitative treatment of these reactions and the comparison with diffractive data

We will consider reactions of the type illustrated in fig. 1 where a reggeon exchange production mechanism has been assumed. The meson resonance M* will usually be taken from the four $L = 1$ quark model nonets, although we briefly consider some examples of $L = 2$ resonances (for example, the $3^-(g)$ nonet – the Regge recurrence of the ρ meson). The $L = 1$ nonets contain the lowest-lying examples of controversial resonances which cannot be produced by π-exchange. The dynamics of π-exchange processes are well known [5], and, apart from an interesting application

* Supported by the US Atomic Energy Commission, San Francisco Operations Office
** Present address CERN, Geneva, Switzerland

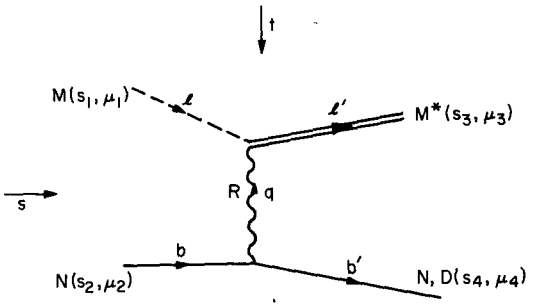

Fig 1. Diagram representing production of a meson resonance M* by exchange of reggeon R from an incident 0^- particle M N represents the target nucleon The recoil particle will be taken from the $L = 0$ quark model ground state ($1/2^+$ N octet or $3/2^+$ D decuplet) s_t is the spin and μ_t the s-channel helicity s and t are the usual invariants and four-momenta, l, l', b, b' and q are used in the text (subsect 3 5, sect 5, and appendix B).

to A_1 and B photoproduction in sect. 7, we will not study them in this paper.

The organization of the paper is as follows· First, in sect. 2 we define the meson states – both purported and supported – whose production we will study. Then, in sect. 3, we describe in some detail the theoretical weapons to be used to study our reactions Explicitly, we define our notation for helicity amplitudes and detail our extrapolation ansatz, give the SU(3) and exchange-degeneracy (EXD) constraints, and describe the calculation of meson-resonance radiative decay widths in an explicit quark model [6] Note that two topics were exiled to appendices. These cover details of our pole extrapolation procedure and a summary of the quark model of Feynman, Kislinger and Ravndal [6] as applied to mesons.

Sect. 4, specializing to natural-parity exchange, describes the SU(3) and pole-extrapolation predictions and confronts them with data

In sect. 5, we describe a generalized vector-meson–photon analogy model for vector or tensor Regge couplings, as recently proposed by Kislinger [7] The suppression of 1^+ production cross sections, discovered in sect. 4, is accommodated very naturally in this model. We attempt to subject the model to a more detailed check, using at times quark model predictions for virtual-photon–meson vertices. Unfortunately, even less speculative applications are in poor quantitative agreement with experiment

In sect 6, we consider the (surprisingly) successful predictions of EXD for unnatural parity exchange Meanwhile, hearkening to a different drummer, we find a particularly fine place to study 1^+ production – namely, by π-exchange in photon-induced processes Predictions for these cross sections will be found in sect 7

Sect. 8 contains our conclusions. Further qualitative discussion of our results may be found in ref. [3] and has been omitted from the current paper.

2. The $L = 1$ and 2 quark model states

In table 1, we list the four $L = 1$ quark nonets and indicate the possible experimental candidates [8] for the theoretically expected states. As discussed in ref. [3], it is no accident that those particles (κ, ϵ, S*, $K_N^*(1420)$, $f^0(1260)$) that can be produced by π-exchange are quite well understood *. As we show in sect 4, the remaining 2^+ states have comparatively large cross sections and present no mysteries in their production dynamics. In this paper, we concentrate on the one remaining 0^+ particle ($\pi_N(980)$) and the 1^+ particles. Table 2 contains their dominant decay modes taken from either experiment or SU(3) calculations [9, 10, 11]. As usual, some of the entries in tables 1 and 2 require qualification

(i) The C meson seen in $p\bar{p}$ collisions [8] has been tentatively identified as the strange partner of the A_1. This is not a watertight assignment (for example, it may be in the B nonet), and furthermore, the two Q's – hereafter denoted by Q_{A_1} and Q_B – may mix [10, 11] We will, however, ignore such mixing in this paper.

(ii) The $I = 0$ 1^+ mesons are represented only by the D meson seen in $p\bar{p}$ interactions The second $I = 0$ A_1 partner (D′) has been consistently identified with either the E(1422) or the rather shaky M(953) **. There is essentially no experimental information on h or h′ production.

Theoretically, the situation is confused by the different mixing schemes. First, we can have "magic" mixing as exemplified by the ω and ϕ; in this case, we write the $I = 0$ particles M* (magic $-\omega$) and M* (magic $-\phi$) with an obvious notation (M* = D or h). Alternatively, we can have essentially no mixing as exemplified by the η and η', in this case, we write M* (octet) and M* (singlet).

Table 1
$L = 1$ quark states

J^P / isospin	0^+ nonet	1^+ "B" nonet	1^+ "A_1" nonet	2^+ nonet
$I = 1$	π_N (980)	B(1235)	A_1(1070)	A_2(1310)
Strange $I = 1/2$	κ ($\approx$ 1250)	Q_B (1300 → 1400)	Q_{A_1} = C(?) (1240 → 1290)	K_N^*(1420)
$I = 0$ singlet/octet mixing (?)	ϵ ($\approx$ 750)	h (?)	D(1285)	f^0(1260)
	S* (1000)	h′ (?)	D′ = E(1422) ? or M(953) ?	f′(1514)

* There are still some difficulties with the 0^+ nonet but it is not appropriate to dwell on them here

** Rosner and Colglazier classify the D′ as an unmixed singlet partner of the A_1 and identify it with the M(953) reported by Aguilar-Benitez et al [12]

Table 2
0^+, 1^+ meson decays

Particle	Mass (GeV/c)	Decay	Width (MeV/c)	Source of Width
$\pi_N(980)$	0 98	$\pi\eta$	40	(a)
B(1235)	1.235	$\pi\omega$	100	expt
Q_B (see caveat (i))	1 380	$K\rho$	32	(b)
		$K^*\pi$	80	
		$K\omega$	9	
h(octet – ?)	1.01	$\pi\rho$	40	(b)
h(magic–ω – ?)	1 25	$\pi\rho$	330	(b)
h'(magic–ϕ) see caveat (ii)	1 5	$\bar{K}K^* + K\bar{K}^*$	75	(b)
A_1	1.07	$\pi\rho$	140	"expt" – see caveat (iv)
Q_{A_1} = C (see caveat (i))	1 24	$K\pi\pi$	50	(c)
D(1285)	1 285	$\eta\pi\pi$	$\Gamma_{tot} = 21 \pm 10$	expt
		$K\bar{K}\pi$		
D'(magic–ϕ) = E (?)	1 422	$\bar{K}K^* + K\bar{K}^*$	50	(c)
D' (singlet)	any	$\bar{K}K^* + K\bar{K}^*$	0	(c)

Sources (a) SU(3) and $\epsilon \to \pi\pi$ = 300 MeV, (b) SU(3) and B $\to \pi\omega$ = 100 MeV, (c) SU(3) and $A_1 \to \pi\rho$ = 140 MeV Caveats are expounded in sect 2

Duality schemes predict h, h' to have magic mixing and D, D' to be unmixed [13] The naive quark model predicts exactly the opposite *, here we can only consider all possibilities

(iii) For the 0^+ mesons, if the κ is indeed the heaviest member of the nonet, then no mixing angle can be found to fit the mass formulae [9]

(iv) Note that the A_1 nonet parameters in table 2 are perhaps a little dubious since they are normalized to an A_1 mass and width derived from diffraction data, and there are reasons to believe such parameters to be unreliable [3] (Similar objections, of course, apply to the Q parameters.) However, comparable results are given using the quark model to relate the A_1 and B couplings [6, 10, 11]. Quantitative ** quark prediction for A_1 width does, however, depend on its mass, for instance, an

* In the model of ref. [6], the B nonet is an orbital excitation of the π nonet and so unmixed The A_1 being an $L = 1$ excitation of the ρ has magic mixing. However, the duality arguments of ref. [13] give the opposite result

** See formulae in appendix A and table 17

A_1 mass of 1.285 GeV (equal to that of the D meson) would increase its expected width to over 200 MeV *. Such mass changes (1.07 to 1 285) are allowed because current theories of SU(3) mass breaking are quite phenomenological.

We must, of course, bear these and other caveats in mind, during the succeeding sections. However, they are not a major difficulty – indeed, an important motivation for the theoretical models and estimates to follow is the prediction of cross sections so that experiments can be designed to determine such ambiguous or unknown resonance parameters.

Finally, we note that, at times, we will treat the $L = 2$ quark states These are expected to consist of nonets with $J^{PC} = 2^{-+}$, 1^{--}, 2^{--}, and 3^{--}. The $I = 1$ members we will respectively denote by A_3, ρ', A_1^* (as it is EXD friend of A_1 – maybe A_1^* is the $F_1(1540)$ state [8]), and g. The $I = 0$ member of the 3^- nonet with ω-like mixing is identified with the perversely named $\phi_N(1680)$, ref. [8].

3. Theory

Here we detail the basic theoretical formulae to be used in the following. Subsects. 3.1–3.3 have the pole-extrapolation, SU(3), EXD and factorization ideas used in the natural parity exchange [we denote this V (for vector, e.g., ρ, ω ..) and T (for tensor, e.g., A_2, f^0 ..) hereafter] data comparison in sect 4. Subsect 3.4 is a comparable discussion for unnatural parity exchange – see sect 6 for the corresponding data comparison. Subsect. 3.5 gives the quark model estimates [6] for meson radiative decays We use this in both quantitative calculations in Kislinger's [7] generalized vector-meson–photon analogy model (sect. 5) and in predicting the photoproduction of 1^+ particles (sect 7). So after this sop to a global overview, we plunge into a morass of technical detail

3 1. Pole extrapolation

We first define some necessary helicity-amplitude notation Describe the reaction $1 + 2 \to 3 + 4$ by s-channel helicity amplitudes $H_s^{\mu_3\mu_4\ \mu_2\mu_1}(s, t)$ where s and t are the usual invariants (see fig. 1) and μ_i are the respective s-channel helicities Our normalization is such that

$$\frac{d\sigma}{dt} = \frac{0\,3893}{64\pi m_2{}^2 P_{\text{lab}}^2} \sum{}' |H_s^{\mu_3\mu_4\ \mu_2\mu_1}|^2 \text{ mb/(GeV/}c)^2, \tag{1}$$

where Σ' is the usual spin-averaged helicity sum and m_2 the target mass.

The expression for the helicity amplitudes corresponding to the exchange of a Regge pole with trajectory $\alpha(t)$ is up to an irrelevant sign [14]

$$H_s^{\mu_3\mu_4\ \mu_2\mu_1} = \frac{V(t)}{\sin \pi\alpha}\, \alpha'\, s^{\alpha(t)}\, g_{\mu_3\mu_1}(t)\, g_{\mu_4\mu_2}(t)\, \overline{\text{PRB}}\,(s, t). \tag{2}$$

* See formulae in appendix A and table 17

Here.

(i) $g_{\mu_i\mu_j}(t)$ are the s-channel residues. In our case, $g_{\mu_2\mu_4}$ is a baryon-baryon residue known from factorization [see table 6]. Particle 1 is the 0^- incident meson and 3 the resonance. So $g_{\mu_3\mu_1}$ is known at the pole $t = m_V{}^2$ from the width of particle 3. We give the explicit formulae in appendix A. Again, we specify the "natural" pole extrapolation as

$$g_{\mu_3\mu_1}(t) = (\sqrt{t}/m_V)^{|\mu_3-\mu_1|}\, g_{\mu_3\mu_1}(m_V{}^2) \tag{3}$$

for the relative t-dependence of the different amplitudes. Eq (3) gives to g the minimum t-dependence implied by an evasive (Toller quantum number $M = 0$) Regge pole g has no other kinematic singularities or zeros. Eq. (3) specifies our assumption of a smooth pole extrapolation. Rather, to be exact, as we only look at amplitude ratios, we assume any other t-dependence (e.g., an intrinsic exponential, see eq. (9)) is independent of the produced particle.

(ii) α', the slope of the Regge trajectory, is inserted for later convenience so that the couplings g in eq. (1) are correctly [14] converted from residues in the j-plane to those in the m^2-plane. This conversion is tacitly assumed in the above discussion (i) and in the explicit formulae of appendix A

(iii) $V(t)/\sin\pi\alpha$ is the signature factor Specializing to vector/tensor exchange, it is again convenient to normalize it so that $V(m_V{}^2) = 1$ for the negative signature (component of the) Regge pole Here m_V is the mass of the first 1^- particle on the trajectory. Details are given in table 3.

Table 3
Signature factors

Label in tables 4 and 5	Explicit form
V_1	$\frac{1}{2}[1 - \cos\pi\alpha + i\sin\pi\alpha]$
V_2	$-\cos\pi\alpha + i\sin\pi\alpha$
V_3	1
V_4	$-\frac{1}{2}[1 + \cos\pi\alpha - i\sin\pi\alpha]$
V_5	$\frac{1}{6}[2 - 4\cos\pi\alpha + 4i\sin\pi\alpha]$
V_6	$\frac{1}{2}[-2 - 4\cos\pi\alpha + 4i\sin\pi\alpha]$

The six signature factors to be used in eq (2) together with the isoscalar factors in tables 4 and 5 The latter detail the correspondence between the six factors and particular vertices V_i are multiplied by the isoscalar factor for V exchange unless this is zero when you use the T exchange entry Note these forms are *only* valid in the simple EXD quark world discussed in subsect 3 2.

(iv) $\overline{\mathrm{PRB}}(s, t)$ ensures that H_s has the correct kinematic behaviour at the physical region boundary and is ingeniously normalized so that $\overline{\mathrm{PRB}}(s, t) \to 1$ as $s \to \infty$ at fixed $t \neq 0$, i.e.,

$$\begin{aligned}
&\overline{\mathrm{PRB}}(s, t) = x_1^{\frac{1}{2}|\mu_1 - \mu_f|} x_2^{\frac{1}{2}|\mu_1 + \mu_f|}, \\
&x_1 = \tfrac{1}{2}(1 - \cos\theta_s)\nu/-t, \qquad x_2 = \tfrac{1}{2}(1 + \cos\theta_s), \\
&\nu = \tfrac{1}{2}(s - u), \quad \theta_s = s\text{-channel c.m.s. scattering angle}, \\
&\mu_1 = \mu_1 - \mu_2, \qquad \mu_f = \mu_3 - \mu_4.
\end{aligned} \tag{4}$$

3 2. SU(3), EXD and factorization. V, T exchange for meson vertices

Consider the vertices $g_{\mu_1 \mu_3}$ for 0^- (helicity $\mu_1 = 0$) goes to M* (helicity μ_3) by V or T exchange. SU(3) relates these couplings for different M*'s in the same multiplet. For a given nonet of M*'s, we can write the predictions in terms of $g(8, \mathrm{V})$, $g(1, \mathrm{V})$, $g(8, \mathrm{T})$, and $g(1, \mathrm{T})$ where 8/1 labels the octet/singlet M* couplings and V/T the vector/tensor exchanged trajectory. Table 4 records the SU(3) isoscalar coefficients for M* = B and table 5 for the opposite charge conjugation M* = A_1. The tables can also be used for the π_N and A_2 nonets with changes in particle nomenclature The coupling, for given charge states, is the relevant $g(8/1, \mathrm{V/T}) \otimes$ table 4, V/T factor $\otimes$ SU(2) Clebsch-Gordan coefficient for $3 \to 1 + \mathrm{V, T}$. For the isosinglet mesons, we designate the pure singlet/octet particles as $M_{1,8}$ and for the magic mixing combinations, we write

$$M_\omega = (\sqrt{2}\, M_1 + M_8)/\sqrt{3}, \qquad M_\phi = (M_1 - \sqrt{2}\, M_8)/\sqrt{3}. \tag{5}$$

Now we can further reduce our parameters – with the sign convention that V exchange has signature factor proportional to $-\frac{1}{2}(-1 + e^{-i\pi\alpha})$ and T proportional to $-\frac{1}{2}(1 + e^{-i\pi\alpha})$ (see table 3). Then duality (EXD) implies $\mathrm{KN} \to (A_1, \mathrm{B})\mathrm{N}$ is real and from tables 4 and 5 this implies

$$g(8, \mathrm{V}) = g(8, \mathrm{T}). \tag{6}$$

Further the naive quark model rules (i.e., no disconnected graphs) imply

$$g(1, \mathrm{V}) = g(8, \mathrm{V}), \qquad g(1, \mathrm{T}) = g(8, \mathrm{T}); \tag{7}$$

eq. (7) is only expected to be reasonable for magically mixed nonets. The only unmixed nonet studied occurs when we take M* as the 0^- nonet. Here Martin and Michael [15] find from η and η' production data that

$$g(1, \mathrm{V/T}) \approx \tfrac{1}{2}\, g(8, \mathrm{V/T})$$

and a mixing angle for η_1 and η_8 which tends to increase the factor of 2 reduction of the amplitude for the (dominantly) SU(3) singlet η' particle. The situation is confused and not understood Further, as pointed out in the introduction, we do not even know what is the correct mixing scheme for the 1^+ mesons. So in the following,

Table 4
SU(3) isoscalar factors for the B nonet

Particle 3	Vertex 1	V	Value	Vertex 1	T	Value	Net signature factor
B	π	ρ	0	π	A_2	−2	V_4
	π	ω	$\sqrt{2}$	π	f_0	0	V_1
	$\bar{K}$	K*(890)	−1	$\bar{K}$	K*(1400)	1	V_3
$\bar{Q}_B$	$\bar{K}$	ρ	$-\sqrt{3/2}$	$\bar{K}$	A_2	$-\sqrt{3/2}$	V_2
	$\bar{K}$	ω	$1/\sqrt{2}$	$\bar{K}$	f_0	$1/\sqrt{2}$	V_2
Q_B	π	K*(890)	$-\sqrt{3/2}$	π	K*(1400)	$-\sqrt{3/2}$	V_2
	K	ρ	$\sqrt{3/2}$	K	A_2	$-\sqrt{3/2}$	V_3
	K	ω	$1/\sqrt{2}$	K	f_0	$-1/\sqrt{2}$	V_3
h_ω	$\bar{K}$	K*(890)	1	$\bar{K}$	K*(1400)	−1	V_3
	π	ρ	$-\sqrt{6}$	π	A_2	0	V_1
h'_ϕ	$\bar{K}$	K*(890)	$\sqrt{2}$	$\bar{K}$	K*(1400)	2	V_2
	π	ρ	0	π	A_2	0	
h_8	$\bar{K}$	K*(890)	$-1/\sqrt{3}$	$\bar{K}$	K*(1400)	$-\sqrt{3}$	V_6
	π	ρ	$-\sqrt{2}$	π	A_2	0	V_1
h_1	$\bar{K}$	K*(890)	$2\sqrt{2/3}$	$\bar{K}$	K*(1400)	0	V_1
	π	ρ	−2	π	A_2	0	V_1

(i) These SU(3) isoscalar factors differ by an irrelevant overall factor from those in de Swart [45]
(ii) The signature factors $V_{1\to 6}$ are given in table 3
(iii) Unnatural-parity exchange couplings are given by the replacement V to B, T to π nonet

we shall always take the simple result implied by eqs. (6) and (7), i.e

$$g(1, V) = g(1, T) = g(8, V) = g(8, T) \tag{8}$$

Given this, it is convenient to note that, in any reaction of the type in fig 1, the net signature factor (V + T) takes one of the six forms in table 3.

3.3. SU(3), EXD and factorization: V, T exchange for baryon vertices

Let N denote any member of the lowest-lying $\frac{1}{2}^+$ baryon octet * and D any member of the standard $\frac{3}{2}^+$ decuplet. Then the study of the simple PN → P(N, D) reactions (here P is any member of the pseudoscalar nonet), has isolated the values of

* We will sometimes use N to denote the nucleon rather than a general member of the $\frac{1}{2}^+$ octet Our meaning will always be obvious in context

Table 5
SU(3) isoscalar factors for the A_1, (A_2 and $\pi_N(980)$) nonets

Particle 3	vertex 1	V	Value	vertex 1	T	Value	Net signature factor
	π	ρ	-2	π	A_2	0	V_1
A_1	$\bar{K}$	K*(890)	1	$\bar{K}$	K*(1400)	-1	V_3
	π	ω	0	π	f_0	$\sqrt{2}$	V_4
	$\bar{K}$	ρ	$-\sqrt{3/2}$	$\bar{K}$	A_2	$-\sqrt{3/2}$	V_2
$\bar{Q}_A$	$\bar{K}$	ω	$1/\sqrt{2}$	$\bar{K}$	f_0	$1/\sqrt{2}$	V_2
	π	K*(890)	$-\sqrt{3/2}$	π	K*(1400)	$-\sqrt{3/2}$	V_2
Q_A	K	ρ	$-\sqrt{3/2}$	K	A_2	$\sqrt{3/2}$	V_3
	K	ω	$-1/\sqrt{2}$	K	f_0	$1/\sqrt{2}$	V_3
D_8	$\bar{K}$	K*(890)	$-\sqrt{3}$	$\bar{K}$	K*(1400)	$-1/\sqrt{3}$	V_5
	π	ρ	0	π	A_2	$-\sqrt{2}$	V_4
D_1	$\bar{K}$	K*(890)	0	$\bar{K}$	K*(1400)	$2\sqrt{2/3}$	V_4
	π	ρ	0	π	A_2	-2	V_4
D_ω	$\bar{K}$	K*(890)	-1	$\bar{K}$	K*(1400)	1	V_3
	π	ρ	0	π	A_2	$-\sqrt{6}$	V_4
D_ϕ	$\bar{K}$	K*(890)	$\sqrt{2}$	$\bar{K}$	K*(1400)	$\sqrt{2}$	V_2
	π	ρ	0	π	A_2	0	

(i) These SU(3) isoscalar factors differ by an irrelevant overall factor from those in de Swart [45].
(ii) The signature factors $V_{1\to6}$ are given in table 3
(iii) The couplings are written out for the A_1 nonet. Replacing A_1 by corresponding A_2 nonet members gives the latter's couplings Replacing A_1 by $\pi_N(980)$, V by B nonet, T by π nonet gives the unnatural-parity exchange $\pi_N(980)$ couplings
(iv) In fact, for A_1, A_2 unnatural-parity exchange, we need only make the same replacement V to B, T to π nonet

$g_{\mu_2\mu_4}(t)$ for the V, T → N($\bar{N}$, $\bar{D}$) vertices [16, 17] Of course, our knowledge of these g in overall size and t dependence is not uniformly good for all N and D multiplet members. However, it is not appropriate to discuss this here, nor is it necessary. Thus, our estimates will be sufficiently crude (i.e. they are hopefully valid to around a factor of two), that niceties of specific knowledge are not relevant. In particular, we will completely ignore absorption corrections [16, 18]. This can be justified (rationalized) by both the resultant simplicity of the consequent pole-only description and also the unfortunate fact that we simply do not know how to formulate a quantitative absorption model for these complex reactions. This defect (i.e., omission of absorption corrections) can be partially compensated by regarding the Regge estima-

Table 6
Baryon couplings

Vertex	Helicity state	Value
$(f^0)\omega \to N\bar{N}$	g_{++}	-4
	g_{+-}	0
$(A_2)\rho \to N\bar{N}$	g_{++}	-1
	g_{+-}	$-4\sqrt{-t}$
$(K^{**})K^* \to N\bar{\Sigma}$	g_{++}	$-1\ 9$
	g_{+-}	$2\ 44\sqrt{-t}$
$(K^{**})K^* \to N\bar{\Lambda}$	g_{++}	$-1\ 2$
	g_{+-}	$-2\ 44\sqrt{-t}$
$(A_2)\rho \to N\ \bar{\Delta}(1234)$	$g_{\mu_2\mu_4}$	$6\ S_{\mu_2\mu_4}\sqrt{-t}$
$(K^{**})K^* \to N\bar{Y}^*(1385)$	$g_{\mu_2\mu_4}$	$10\ S_{\mu_2\mu_4}\sqrt{-t}$

The values of $g_{\mu_2\mu_4}$ to be used in eq (2) with the parameterization described in subsect 3 3 $S_{\mu_2\mu_4}$ is given in eq (12)

tes, in the following, as "effective" pole (+ cut) contributions. However, this is not really satisfactory, as we shall use factorization to relate reactions of different spin-structures and doing this with "effective" poles ignores completely the spin-dependence of absorption [16, 18].

So, bearing in mind the above caveats, we record in table 6, the values we shall use in the succeeding sections for $g_{\mu_2\mu_4}$. These numbers are normalized so that they give reasonable fits to PN → P(N, D) $d\sigma/dt$ data when combined with the values of $g_{\mu_1\mu_3}$ (V, T → PP) recorded in eq. (59) of appendix A. As usual (in this paper), the numbers in table 6 must be multiplied by an SU(2) Clebsch-Gordan coefficient to find the amplitude for a given charge state; this time it is the coefficient appropriate for V, T → 2, $\bar{4}$. Not only this, but an extra, and entirely phenomenological, t-dependent factor is necessary. This turns out to be

$$f = \frac{4.6}{\Gamma(\alpha)} \exp[a_i t'], \tag{9}$$

where the peripheralizing a_i were chosen to be 3·5 for total s-channel non-flip ($n = |\mu_1 - \mu_f| = 0$ in eq. (4)) and 1.0 for the remaining amplitudes.

t' in eq. (9) is, as usual, $t - t_{min}$ where $t = t_{min}$ is the physical region boundary. The use of t' rather than t in eq. (9) – *a priori* either is reasonable – improves agreement with data at low energy. (They are the same asymptotically.)

Again, we note that we use conventional V, T trajectories, i.e

$$\begin{aligned} &\rho, A_2, \omega, f^0: && \alpha(t) = 0.5 + 0.9t \\ &K^*, K^{**} && \alpha(t) = 0.35 + 0.9t. \end{aligned} \tag{10}$$

The spin-dependence of V, T → NN̄ couplings in table 6 is denoted by the "unit" vector $S_{\mu_2\mu_4}$ whose four (independent) members are normalized by

$$|S_{\frac{1}{2}-\frac{3}{2}}|^2 + |S_{\frac{1}{2}-\frac{1}{2}}|^2 + |S_{\frac{1}{2}\frac{1}{2}}|^2 + |S_{\frac{1}{2}\frac{3}{2}}|^2 = 1. \tag{11}$$

The helicity dependence of S is irrelevant for $d\sigma/dt$ but is constrained by the experimental observation of a dip in $d\sigma/dt$ at $t = 0$ (i.e. $S_{\frac{1}{2}\frac{1}{2}}(t = 0) = 0$) and the Stodolsky-Sakurai decay distribution for the decuplet. S is certainly not uniquely determined by this, for instance, it is rotation invariant [16]. However, a reasonable choice is

$$S_{\frac{1}{2}-\frac{3}{2}} = S_{\frac{1}{2}\frac{1}{2}} = 0, \qquad S_{\frac{1}{2}-\frac{1}{2}} = \tfrac{1}{2}, \qquad S_{\frac{1}{2}\frac{3}{2}} = \tfrac{1}{2}\sqrt{3}, \tag{12}$$

where most people would like eq (12) to be true for t-channel helicities.

The quality of the representation of PN → P(N, D) data by the symbolic parameterization described in this section is indicated in fig. 2 *. The poor agreement be-

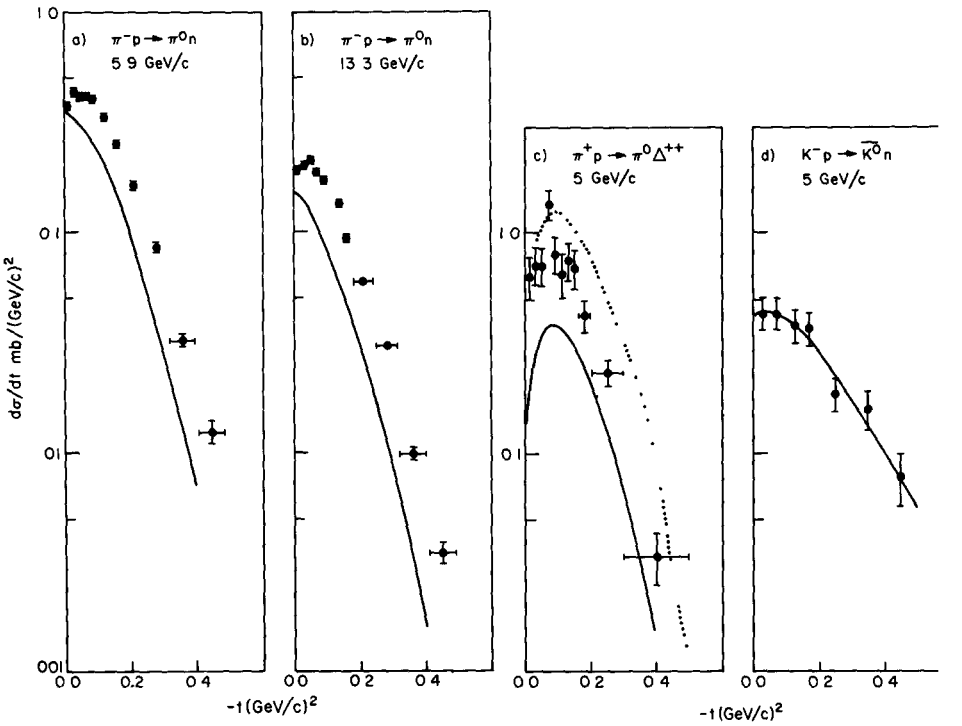

* The ω/f^0 exchange parameters are not tested in fig 2 The ω/ρ ratio comes from total cross sections, $K^0_L p \to K^0_S p$ data and the ratio of $K^{\pm}p \to K^{\pm *}p$ to $K^{\pm}n \to K^{\pm *}n$

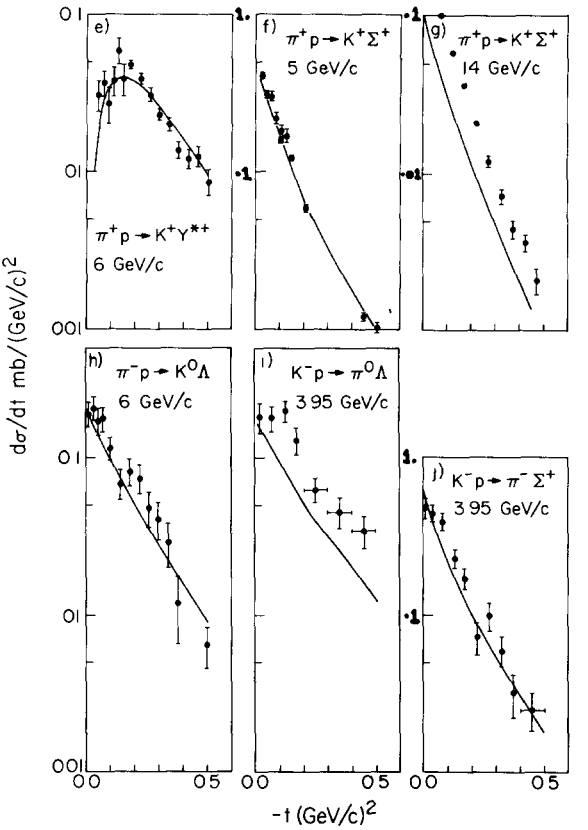

Fig 2 Comparison of the simple parameterization of subsect 3 3 (solid curve) with experimental data from refs (a), (b), [19], [20]. (c), [21] (d), [22] (e), (g), [23] (f), [24], [25] (h), [26] (i), (j), [27] An indication of the danger of "universal" parameters is the dotted line in (c) which uses instead of eq (10), $\alpha_\rho(t) = 0\,58 + t$ and reduces the a_i in (9) by 1, otherwise, the parameterization is identical to that described in subsect 3 3 and represented by the solid curve in (c).

tween theory and experiment can be traced to violation of EXD around 5 GeV/c ($K^-p \to \pi^-\Sigma^+$ somewhat larger than $\pi^+p \to K^+\Sigma^+$, $K^-p \to \pi^0\Lambda$ larger than $\frac{1}{2}(\pi^-p \to K^0\Lambda)$), failure of Regge energy dependence (compare $\pi^+p \to K^+\Sigma^+$ at 6 and 14 GeV/c), and inadequacy of "universal" parameters ($\pi^-p \to \pi^0n$ can be fitted much better than fig. 2 with Regge-pole model)

3 4 SU(3), EXD and factorization· Unnatural-parity exchange

In a perfect world (full of dreaming spires and beloved of theorists), the treatment of unnatural-parity exchange would be identical to the natural parity (V, T) discussion of subsect. 3.2. Thus, neglect A_1 (and its EXD friend) nonet exchange

There is evidence *for* this from $\pi^- p \to \rho^0 n$ data [28, 29] and *against* from both hypercharge-exchange reactions (the analysis of ref. [30] needed sizable Q_{A_1} exchange) and polarization seen in $\pi^- p \to (\pi^0\pi^0)n$ [31]. We will not dwell on such murky matters but rather consider just the exchange of π and B nonets. As in subsect 3.2, we introduce four couplings $g(8/1, \pi/B)$ with SU(3) isoscalar factors given in tables 4 and 5. Again, we ignore the SU(3) singlet ambiguity and place

$$g(8, \pi/B) = g(1, \pi/B). \tag{13}$$

If EXD were correct, we would also have

$$g(8, \pi) = g(8, B). \tag{14}$$

This relation has been tested by comparison of $\pi^- p \to \omega^0 n$ with $\pi^- p \to \rho^0 n$ and $\pi^+ p \to \omega^0 \Delta^{++}$ with $\pi^+ p \to \rho^0 \Delta^{++}$ [32]. The $\rho - \omega$ interference effect in the latter reaction confirms the sign and phase prediction [33] of eq. (14). However, the magnitude of the differential cross sections show that eq. (14) underestimates the B amplitude by a factor of 1.5 to 2. Let us express this discrepancy·

$$g(8, \pi)/g(8, B) = \gamma \tag{15}$$

where the above data gives γ for the π, B → PV vertex We consider it most reasonable that for the general π, B → PM* vertex, one should assume that γ is not equal to its EXD value 1 but takes on a value independent of the produced meson M*. In practice this implies that we find from experiment the ratio of π couplings

$$g(8, \pi)\big|_{\pi \to PM^*} \text{ to } g(8, \pi)\big|_{\pi \to PV}$$

for any M* nonet and then predict the B, K, Q_B exchange M* reactions by multiplying the corresponding (i.e same exchange) V production reaction by the π-exchange ratio. In the case where the M* and V nonets have opposite charge conjugation, this is (trivially) modified by Clebsch-Gordan coefficients determinable from tables 4 and 5. Symbolically we can summarize our prediction as

$$\mathrm{PN} \to \mathrm{M_1{}^*N}\Big|_{\substack{\text{"B-nonet"}\\ \text{exchange}}} = \mathrm{PN} \to \mathrm{V_2N}\Big|_{\substack{\text{"B-nonet"}\\ \text{exchange}}} \tag{16}$$

$$\otimes \frac{\mathrm{PN} \to \mathrm{M_3{}^*N}\Big|_{\substack{\pi\\ \text{exchange}}}}{\mathrm{PN} \to \mathrm{V_4N}\Big|_{\substack{\pi\\ \text{exchange}}}} \otimes \text{Clebsch-Gordan factor}^2.$$

Here M^*_i are different members of the same SU(3) meson resonance multiplet, V_2, V_4 are members of the ground state ρ, ω nonet. To use (16), we must have as input, V production data by B nonet exchange. These are summarized in table 7 [34–37, 40] and illustrated in figs 3 and 4 Thus, choosing a representative experiment in each case, we accumulate $(\rho_{00} + \rho_{11} - \rho_{1-1})d\sigma/dt$ for both B exchange (fig 3) [34, 35] and K − Q_B exchange (fig 4) [36, 37] The following comments are in order.

Table 7
Parameterization of unnatural-parity exchange around 5 GeV/c

Exchange	Reaction	P_{lab}	$(\rho_{00}+\rho_{11}-\rho_{1-1})d\sigma/dt$ (mb/(GeV/c)^2)
B	$\pi^+n \to \omega^0 p$	5	$0.35\, e^{2t}$
B	$\pi^+p \to \omega^0 \Delta^{++}$	5	$0\,6\ e^{2t}$
K–Q_B	$K\,N \to (\omega, \rho, \phi)\Sigma$	~ 5	0
K–Q_B	$K^-p \to (\rho, \omega)\Lambda$ = $\frac{1}{2}(K^-p \to \phi\Lambda)$ = $\frac{1}{2}(\pi^-p \to K^*(890)\Lambda)$	3 9	$0\,047\, e^{2t}$
K–Q_B	$\frac{1}{2}(K^-p \to \rho^- Y^{*+}(1385))$	3 9 *	$0.09\ e^{3t}$
K–Q_B	$\frac{1}{2}(K^-p \to \rho^- Y^{*+}(1385))$	5·5 *	$0\,024\, e^{3t}$

* We average these as $0\,077\, e^{3t}\,(p_{lab}/3.9)^{-3}$

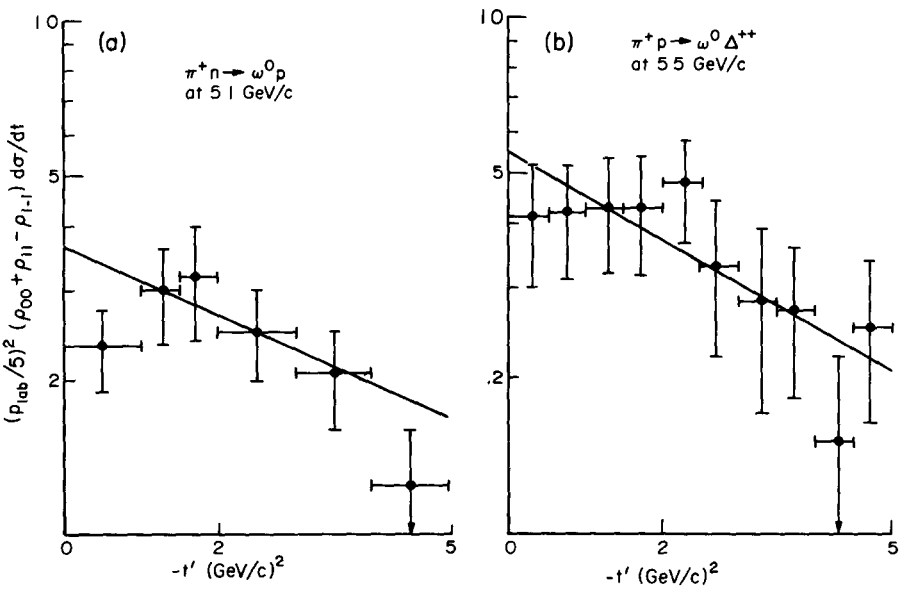

Fig 3. $(p_{lab}/5)^2\,(\rho_{00}+\rho_{11}-\rho_{1-1})d\sigma/dt$ representing the unnatural-parity exchange part of ω production in (a) $\pi^+n \to \omega^0 p$ (ref. [34]) and (b) $\pi^+p \to \omega^0\Delta^{++}$ (ref [35]). The parameterizing curves are summarized in table 7

(i) We do not include any Σ data, e g., $K^-p \to (\omega, \rho)\Sigma$, because in agreement with our prejudice about a small $K \to N\bar{\Sigma}$ coupling, there is little evidence for unnatural parity exchange in such reactions. Trivially, we then predict the same lack of unnatural-parity exchange in all $KN \to M^*\Sigma$ processes. Although this agrees with current data, it is not stringently tested.

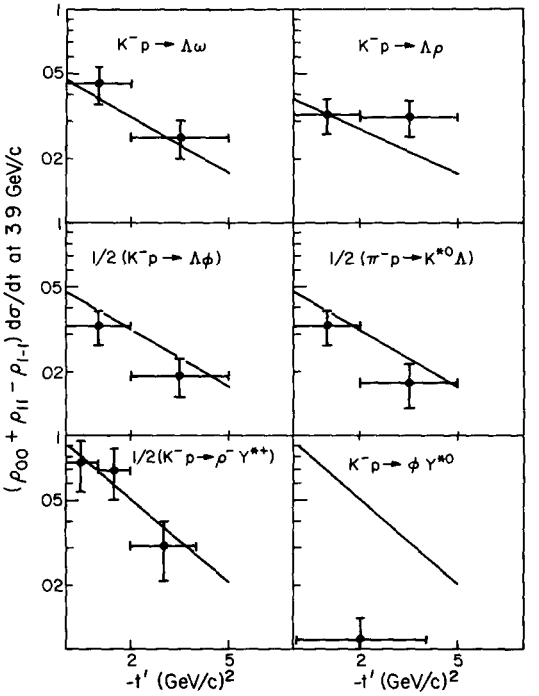

Fig. 4 $(\rho_{00} + \rho_{11} - \rho_{1-1})d\sigma/dt$ for vector-meson production by unnatural-parity hypercharge exchange. The data for the six reactions in the figure are from refs [36, 37] The parameterizing curves are discussed in subsect 3.4, and summarized in table 7

(ii) One may wax eloquent for many a moon on the standard folklore applied to the hypercharge-exchange reactions in fig. 4. Here, rather than a full core dump, we present a restrained soliloquy.

SU(3) predicts the equality of $K^-p \to \rho\Lambda$ to $K^-p \to \omega\Lambda$ and $K^-p \to \phi\Lambda$ to $\pi^-p \to K^*\Lambda$. This agrees with experiment as indicated in fig. 4 and demonstrated by the nice analysis of Aguilar-Benitez et al [36, 38].

Further, EXD predicts $K^-p \to (\rho, \omega)\Lambda = \frac{1}{2}(K^-p \to \phi\Lambda, \pi^-p \to K^*\Lambda)$. This is less successful – the "moving phase" reactions (ϕ and K* production) lying lower than their "real" counterparts (ρ, ω production). A closer examination shows that this effect is even bigger in the natural-parity component of these reactions. This is pleasing for similar systematics are seen in $K^{\pm}p \to K^{*\pm}(890)p$ [39]. However, such line-reversal breaking, although interesting, is just one of those niceties which are irrelevant for our rough estimates.

(iii) It is noteworthy that decuplet production (e.g. $\pi^+p \to \omega^0\Delta^{++}$ and $K^-p \to \rho^-Y^{*+}(1385)$) has a larger unnatural-parity exchange than their octet counter parts (e.g. $\pi^+n \to \omega^0p$, $K^-n \to \rho^-\Lambda$). Invoking a bit of π-B EXD, this can be traced to

the larger $\pi N\bar{\Delta}$ than $\pi N\bar{N}$ coupling. This is particularly clear in $K^-p \to \rho^- Y^{*+}(1385)$ because, in addition, the natural-parity exchange is much smaller than for $K^-n \to \rho^-\Lambda$ (note the $\sqrt{-t}$ for Y*(1385) in table 6). It follows that one predicts that $\rho^- Y^{*+}(1385)$ is all unnatural-parity exchange around 5 GeV/c. This is clearly supported by the data [36, 40–42] compiled in table 8.

$K^-p \to \phi\, Y^{*0}(1385)$ is a fly in the ointment for fig. 4 reveals it to be fully an order of magnitude below the SU(3)/EXD prediction of $\frac{1}{2}$ ($K^-p \to \rho^- Y^{*+}(1385)$) One could attempt to explain this as a combination of.

(a) t_{min} effects the physical region boundary at 3·9 GeV/c for $\phi\, Y^{*0}(1385)$ is -0.18 (GeV/c)^2 while for $\rho^- Y^{*+}(1385)$, it is $-0\,07$ (GeV/c)^2.

(b) $K^-p \to \phi\Lambda$ exhibited some suppression compared with $K^-p \to (\rho, \omega)\Lambda$: thinking of this as a line-reversal breaking ("moving phase" smaller than "real"), we would expect $\phi\, Y^{*0}(1385)$ to be lower than the EXD prediction

(c) Finally, we note that the $\phi\, Y^{*0}(1385)$ data plotted in fig 4 appears a little anomalous, thus, the fraction of unnatural-parity exchange in ϕY^* at 3, 3 15 and 3.3 combined, 3.9 and 4.6 combined, 4.1, 4.48 and 5.5 GeV/c is 0.79 ± 0.13, $0\,85 \pm 0.15$, $0\,32 \pm 0.1$, 0.64 ± 0.25, 0.68 ± 0.14, $0.77 \pm 0\,15$ (respectively, from refs. [43, 44, 36, 40, 41, 40]) The third value, used in fig. 4, is low compared with the other experimental estimates.

One could attempt to clarify the situation by considering $\pi^+p \to K^{*+}(890)\, Y^{*+}$ (1385) which SU(3) predicts to be equal to $K^-p \to \rho^- Y^{*+}(1385)$ However, low statistics and mismatching energies defeat this valiant effort. As recorded in table 8, SU(3) is satisfied at 5 5 GeV/c but the $K^-p \to \rho^- Y^{*+}(1385)$ has a rapid energy dependence from 3.9 to 5.5 GeV/c (which is, however, consistent with the P_{lab}^{-3} behaviour which would not be unreasonable for $K - Q_B$ exchange).

Table 8
Y* production by unnatural-parity exchange *

Reaction	P_{lab}	$\sigma(\mu b)$	$\rho_{00} + \rho_{11} - \rho_{1-1}$	Ref
$K^-p \to \rho^- Y^{*+}(1385)$	3.9	92 ± 8	$0.95 \pm 0\,1$	[36]
	4 6	62 ± 10	$(0 \leqslant \lvert t' \rvert \leqslant 0\,1$ (GeV/c)^2)	[36]
	4.1	70 ± 41	1.17 ± 0.12	[40]
	4.48	10 ± 6	$0\,53 \pm 0.17$	[41]
	5 5	16 ± 7	$1\,12 \pm 0\,06$	[40]
$2(K^-p \to \phi Y^{*0}(1385))$	3.9	40 ± 10	$0\,32 \pm 0\,1$	[36]
	4.6	36 ± 8		[36]
	4.1	24 ± 24	$0.64 \pm 0\,25$	[40]
	4.48	18 ± 3	$0\,68 \pm 0\,14$	[41]
	5 5	18 ± 10	$0\,77 \pm 0.15$	[40]
$\pi^+p \to K^{*+}(890)Y^{*+}(1385)$	5.5	21 ± 4	$0.7 \pm 0\,1$	[42]

* Lower energy data (e g refs. [43, 44]) omitted from table

3.5. Quark model calculation of meson resonances radiative decay widths

To subject Kislinger's model for vector reggeon couplings to a quantitative test, it is necessary to know the amplitudes for virtual photoproduction of meson resonances M* from "ground state" pseudoscalar mesons M; these are related to the matrix elements for radiative decay $M^* \to M + \gamma(q^2)$. The matrix elements involving real photons are also needed for our photoproduction one-pion exchange predictions in sect. 7. Since no experimental information is available on these processes (apart from the $\omega \to \pi\gamma$ decay), one must needs resort to a model. We choose to calculate these matrix elements in the quark model of Feynman, Kislinger and Ravndal [6] (FKR). We could, of course, use the familiar non-relativistic quark model as expounded for baryons by, for example, Copley, Karl and Obryk [46]. However, for photoproduction of nucleon resonances, the two models yield very similar results. There may be significant differences in electroproduction [47, 48] and further both may indeed be wrong for such processes [49]. Anyhow, we shall support the local team who concentrated primarily on baryon-resonance production.
The calculation for mesons is not only similar but easier. To make this paper self-contained a brief summary of the FKR model applied to mesons is contained in appendix B.

Let M*, M and $\gamma(q^2)$ have momenta l', l and q, respectively, with $l'^2 = m^{*2}$ and $l^2 = m^2$. Then define F_μ in terms of the current matrix elements * by

$$2\, m^* F_\mu = \langle l | J_\mu | l' \rangle. \tag{17}$$

These amplitudes F_μ will be evaluated in the meson resonance rest frame for the process $M^* \to M + \gamma(q^2)$ where the photon three-momentum Q^* of modulus Q^* is taken along the z-axis and the scalar and longitudinal parts of the current matrix elements are related by the current conservation condition

$$Q^* F_z = \nu^* F_0, \tag{18}$$

where $q = (\nu^*, Q^*)$ in this frame. Thus, we need consider three amplitudes.
$2\, m^* F_0$, the matrix element of J_0, corresponding to the amplitude involving helicity-zero virtual photons; $2\, m^* F_\pm$, the matrix elements of the spherical components of the current, $(J_x \pm iJ_y)/\sqrt{2}$, corresponding to amplitudes involving transverse photons. The labels on $F_{\pm,0}$, therefore, refer to t-channel helicities of the photon, which is then (minus) the helicity of M* as M is spinless.

The results are derived in appendix B and summarized in table 9. In the latter, we write the amplitudes for either the isospin-1 $M^{*+} \to \pi^+\gamma(q^2)$ or the isospin-$\frac{1}{2}$ "K^{*+}" $\to K^+\gamma(q^2)$ – they always have the same numerical coefficients. For positive charge conjugation C nonets, the isosinglet mesons have zero couplings; for negative C, we multiply table 9 by

$$\sqrt{3}, \sqrt{6}, 3, 0 \qquad \text{for} \quad S_8, S_{\bar{1}}, S_{\omega}, S_{\phi} \tag{19}$$

to get isosinglet $S \to \pi^0\gamma(q^2)$ with the four mixing possibilities. These properties are derived using SU(3) and the identification $\gamma = \rho + \frac{1}{3}\omega - \frac{1}{3}\sqrt{2}\phi$.

* Throughout this paper, our states are normalized covariantly by $\langle p | p' \rangle = 2\, E(2\pi)^3 \delta^3(p - p')$

Table 9
Radiative meson decays in the quark model, $M^{*+} \to \pi^+\gamma(q^2)$

J^{PC}	*Quark model* L	S	Isospin 1 M^{*+}	$F_0/4G$	$F_\pm/4G$
1^{+-}	1	0	B^+	$-\delta\tilde{s}/6$	$\tilde{\tau}/6$
0^{++}	1	1	$\pi_N(980)^+$	0	0
1^{++}	1	1	A_1^+	0	$\delta r/4$
2^{++}	1	1	A_2^+	0	$\delta r/4$
2^{-+}	2	0	A_3^+	$\delta^2\tilde{s}/[2\sqrt{3}]$	$\tilde{t}\delta/2$
1^{--}	2	1	$\rho'(?)^+$	0	$r\delta^2/[6\sqrt{60}]$
2^{--}	2	1	A_1^{*+}	0	$r\delta^2/[6\sqrt{12}]$
3^{--}	2	1	g^+	0	$r\delta^2/[6\sqrt{15}]$

Kinematic quantities are defined in eqs (73), (76) and (79) SU(3) related amplitudes discussed in subsect 3.5 $L = 1$, 2 particles are defined in sect 2

4. SU(3) and pole-extrapolation tests. natural-parity exchange for the $L = 1$ states

This was covered very thoroughly in ref [3], and we will not repeat all the arguments given there.

4.1. 2^+ production

Consider the processes $\pi^\pm p \to A_2^\pm p$ around 5 GeV/c. There is large f^0 exchange [50] contribution which from parity conservation is helicity flip at the πA_2 vertex As we will discuss in sect. 6, there is also B exchange (coupling mainly to helicity-zero A_2's), and so here we eliminate both B and a rather scrawny ρ exchange by forming [50]

$$d\sigma_0/dt = \tfrac{1}{2}\, d\sigma/dt\, \{(\pi^+ p \to A_2^+ p) + (\pi^- p \to A_2^- p) - (\pi^+ n \to A_2^0 p)\}. \qquad (20)$$

The data coming from the recent careful partial-wave analysis of the Illinois group [51] is shown in fig. 5. This also gives the parameter-free prediction of the pole-extrapolation model described in subsects. 3 1–3 3 The amazing agreement between theory and experiment [51, 52] is quite embarassing. Although such a wondrous sight must be accidental, a reasonable concord between theory and experiment was to have been expected. Thus, both theoretically and experimentally, this reaction is dominated by the spin-flip amplitude that consistently shows well-nigh perfect Regge pole behaviour (compare $\pi^- p \to \pi^0 n$, $K^- p \to K^{*-} p$, etc.).

Now let us use SU(3) and factorization to calculate all the hypercharge-exchange reactions producing members of the 2^+ nonet. In practice, we just calculate the pole extrapolation predictions but as this model agrees so well with $\pi N \to A_2 N$, this is almost equivalent to just using SU(3) and factorization to relate all 2^+ production

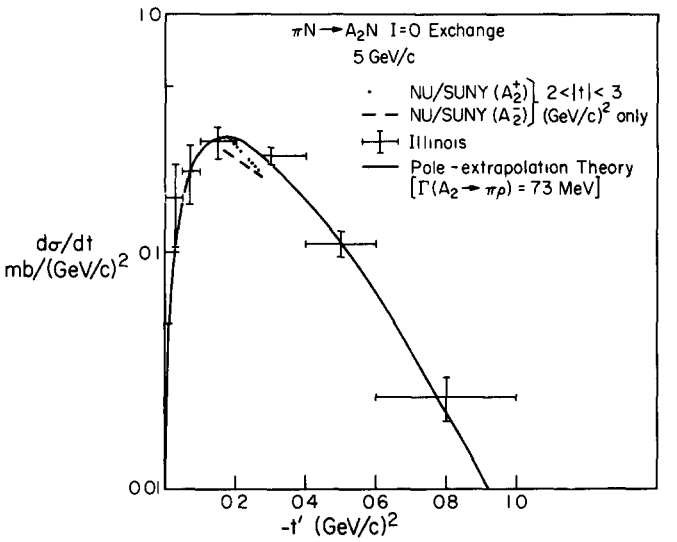

Fig 5 Comparison of the data of refs. [51, 52] for $\pi N \to A_2 N$ with the pole extrapolation model described in subsects. 3.1 and 4 1. The $I = 0$ exchange contribution is defined in eq (20) and $d\sigma/dt$ comes from renormalizing $\pi^{\pm}p \to A_2^{\pm}p$ $d\sigma/dt$ by the ratio of cross sections of the $I = 0$ $\pi N \to A_2 N$ to that of charged A_2 production. (This is given in the compilation in ref [51]) Note that the total A_2 cross sections in ref. [52] should be ignored as they come from an incorrect (as shown by data of ref. [51]) extrapolation of data in $0.2 \leqslant |t| < 0.3$ $(\mathrm{GeV}/c)^2$. The differential cross sections are, however, quite valid as shown in the figure.

to $\pi N \to A_2 N$ *. The experimental and theoretical cross sections are shown in table 10 The reader is horrified, for the theory consistently underestimates the experimental cross sections by anything up to a factor of 4. This is not due either to a failure of SU(3) or even our incompetence – rather it comes from two facts. First, the reactions involving Λ's have sizable unnatural-parity exchange contributions which around 5 GeV/c are bigger than the natural-parity values listed in table 10 (see sect. 6 and take a quick peep at fig. 18). Secondly, only about half the experimental cross section occurs in the range $0 \leqslant -t' \leqslant 1$ $(\mathrm{GeV}/c)^2$ for which the theory is calculated. Unfortunately, the theory is not even reliable past $-t' = 0.5$ and so cannot estimate the whole cross section – again the data is generally not given for a "small" t' cut However, fig. 6 shows a nice comparison of theory and experiment $d\sigma/dt$ (not just production cross section) for $\pi^- p \to K^*(1420)\Sigma^0$. We choose this reaction as the Σ^0 eliminates most of the unnatural-parity exchange while the available of $d\sigma/dt$ removes the second difficulty.

Some of the discrepancies cannot be explained away. One serious technical difficulty is that even, say at 5.5 GeV/c, t_{min} for $K^- n \to f'\Sigma$ is -0.2 $(\mathrm{GeV}/c)^2$, this

* These SU(3) predictions will differ from direct relation of amplitudes at $t = 0$ as the two methods will have different dependence on non-degenerate (SU(3) breaking) mass values.

Table 10
A_2 nonet cross sections *

Reaction	P_{lab}	$\sigma(\mu b)$		Ref
		Theory	Expt	
$\pi^- p \to K^*(1420)\Lambda$	4 5	9 2	29 5 ± 4	[26]
$\pi^- p \to K^*(1420)\Lambda$	6	5 6	11 ± 3	[26]
$\pi^- p \to K^*(1420)\Sigma^0$	4 5	3 8	10 ± 2	[26]
$\pi^- p \to K^*(1420)(\Lambda/\Sigma^0)$	7	6 3	$31 \pm {}^{19}_{7}$	[53]
$K^- p \to A_2^0 \Lambda$	3.9	7 4	23 ± 21	[36]
$K^- p \to A_2^0 \Lambda$	4.1	6 7	< 18	[40]
$K^- p \to A_2^0 \Lambda$	4 6	5 5	23 ± 14	[36]
$K^- p \to A_2^0 \Lambda$	5.5	3 7	< 5	[40]
$K^- n \to A_2^- \Lambda$	4.48	11.1	31 ± 8	[41]
$K^- p \to A_2^- \Sigma^+$	3.5	15	50 ± 13	[54]
$K^- n \to A_2^- \Sigma^0$	4 48	6	13 ± 5	[41]
$K^- p \to f^0 \Lambda^0$	3	14	150 ± 60	[55]
$K^- p \to f^0 \Lambda^0$	3 9	8.1	46 ± 12† (20 ± 10)	[36]
$K^- p \to f^0 \Lambda^0$	4.1	7 3	80 ± 33	[40]
$K^- p \to f^0 \Lambda^0$	4 6	6	60 ± 8† (25 ± 5)	[36]
$K^- p \to f^0 \Lambda^0$	5 5	4	12 ± 5	[40]
$K^- p \to f^0 \Lambda^0$	10 1	1.3	6 ± 5	[56]
$K^- p \to f^0 \Sigma^0$	3	6	110 ± 60	[55]
$K^- p \to f^0 \Sigma^0$	3 9	3 7	25 ± 9	[36]
$K^- p \to f^0 \Sigma^0$	4 6	2 9	15 ± 5	[36]
$K^- n \to f^0 \Sigma^-$	5 5	4	24 ± 7	[57]
$K^- p \to f' \Lambda$	3 9	9.8	7 ± 4	[36]
$K^- p \to f' \Lambda$	4.1	9	22 ± 14	[40]
$K^- p \to f' \Lambda$	4 6	7.7	19 ± 4	[36]
$K^- p \to f' \Lambda$	4 6,5		45	[58]
$K^- p \to f' \Lambda$	5 5	5.4	20 ± 6	[40]
$K^- p \to f' \Lambda$	6	4.7	9 ± 4	[59]
$K^- p \to f' \Sigma^0$	3 9	3.5	0 ± 3	[36]
$K^- p \to f' \Sigma^0$	4.6	3 1	5.3 ± 2	[36]
$K^- n \to f' \Sigma^-$	5 5	1.6	21 ± 3	[57]
$K^- p \to f'(\Lambda/\Sigma^0)$	4.25	13	24 ± 8	[60]

* The well-known $\pi N \to A_2 N$ cross sections are omitted. All cross sections are corrected for unseen decays and the theoretical cross sections were formed by integration from 0 to 1 in $-t'$
† The numbers in brackets give the cross sections in the forward hemisphere.

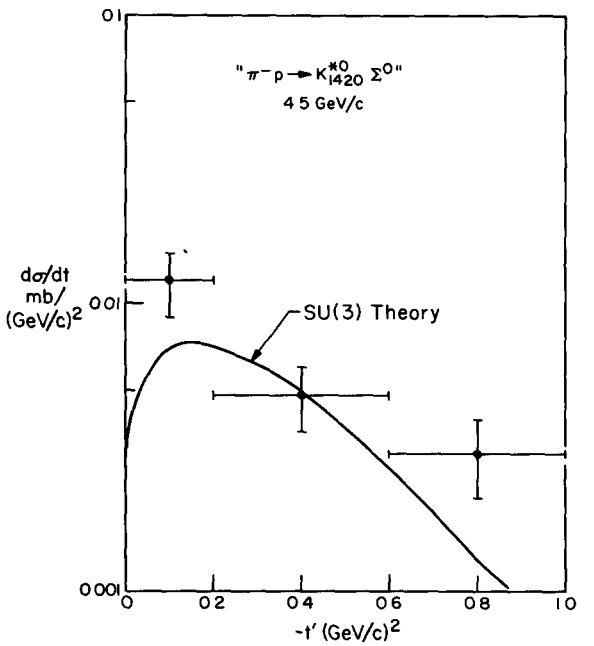

Fig 6 Comparison of $\pi^- p \to K^{*0}(1420)\Sigma^0$ data from ref. [26] with the SU(3) theory expounded in subsect. 4.1. To obtain $d\sigma/dt$ we have cheated somewhat by renormalizing the listed $d\sigma/dt$ for $\pi^- p \to K^{*0}(1420)\Lambda$ by the ratio of production cross sections for $\pi^- p \to K^{*0}(1420)\Sigma^0$ over $\pi^- p \to K^{*0}(1420)\Lambda$. (All data from ref [26].)

physical region boundary suppresses the theoretical cross sections below their naive value. This t_{min} suppression is probably not correctly represented in our formalism, for the difference between the theory and experiment gets particularly bad at low energies where, because of t_{min}, the theory has a slower energy dependence than the simple Regge prediction. The data, if anything, fall faster than Regge as energy increases Further, it would also be nice to find out how much unnatural-parity exchange there really is in the Σ data. If there is violation of the simple rule (no unnatural-parity exchange in Σ production), it will be easier to see in, say $\pi^- p \to K^*(1420)\Sigma'$ (simply because there is generally more unnatural-parity exchange in 2^+ than 1^- production, see sect 6).

Most of the ambiguities described above will be smaller at 15 GeV/c and table 13 lists a selection of predicted cross sections at that energy.

4 2. 1^+ production

Fresh from our stunning triumph with the pole extrapolation model for $\pi N \to A_2 N$, we show a similar comparison for $\pi N \to BN$ in fig. 7. Theory is well over an order of magnitude too big and quite the wrong shape. In fact, the $\pi N \to BN$ data has a simi-

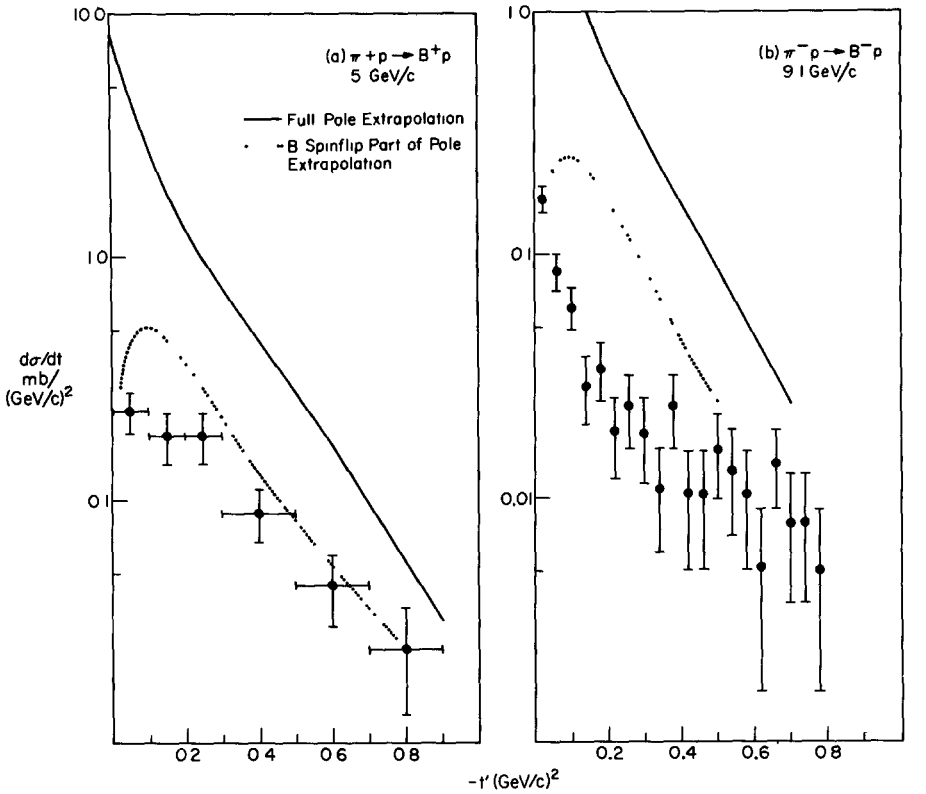

Fig. 7. Comparison of $\pi^{\pm}p \to B^{\pm}p$ data from refs [70, 71] with the pole-extrapolation model described in subsects 3.1 and 4 2 $d\sigma/dt$ comes from normalizing data from a simple mass cut to quoted B cross sections from a Breit-Wigner fit to the whole mass distribution. If the small $|t|$ data is not to be attributed to B production as conjectured in subsect 4.3, this method will be out by up to a factor of 2 in the normalization of the data at larger $|t|$ (even if this is pure B).

lar t dependence to $\pi N \to A_2 N$ and suggests dominance of a spin-flip amplitude. The theory, on the other hand, is mainly non-flip. Thus, both the data and Kislinger's generalized photon-Regge pole analogy to be discussed in the next section, suggest we should drop the non-flip (at the πB vertex) coupling. For this reason, fig. 7 also shows πB spin-flip part of the pole extrapolation prediction. This agrees with the data to within the factor of 2 uncertainty in the model. So it is convenient to define our SU(3) factorization prediction for the *whole* B nonet to be half the spin-flip part of the pole extrapolation value. This is shown in fig 8 for $K^-n \to B^-\Lambda$, theory and experiment [64] agree excellently. Note we do not expect any sizable unnatural-parity contributions to 1^+ production for 1^+ states can only couple in helicity 1 to such an exchange.

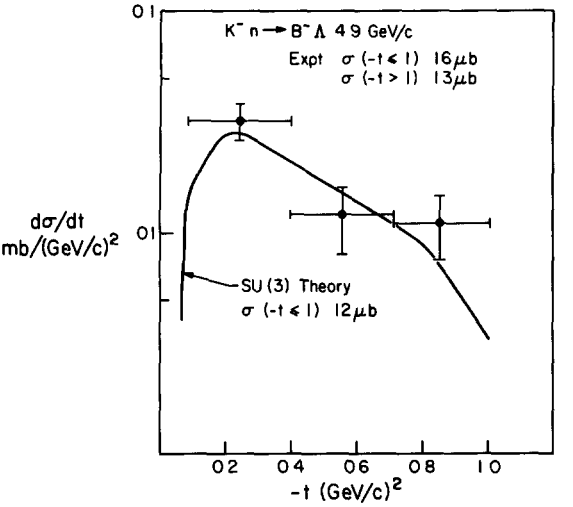

Fig 8 Comparison of $K^-n \to B^-\Lambda$ data at 4.9 GeV/c from ref. [64] with the SU(3) prediction, based on the $\pi N \to BN$ data of the previous figure, and discussed in subsect. 4 2

The largest non-diffractive amplitude producing a member of the A_1 nonet is the f^0 exchange $\pi^\pm p \to A_1{}^\pm p$ Here, of course, we are confused by the much larger diffractive component, and so we must turn to other largish (as there is a healthy $N\bar{\Lambda}$ non-flip coupling) amplitudes $K^-n \to A_1^-\Lambda$ and $\pi^-p \to Q^0\Lambda$. The former is discussed in ref [3], the A_1 may have been seen [72], but the large background precludes a decisive statement. There is a clear Q signal in the second reaction [26], $\pi^-p \to Q^0\Lambda$ at a mass of 1 29 GeV/c and this data is shown in fig 9. Unfortunately, the size of the cross section is quite consistent with this being either the Q belonging to the A_1 or to the B nonet. We assign it to the A_1 nonet, leaving us with no $\pi^-p \to Q_B^0\Lambda$ data for the latter would be at higher mass lurking under the "K*(1420)" signal (see fig 8 of ref. [3]) This assignment, as shown in fig 9, is consistent with the same definition (i.e., one half the spin-flip part of the pole extrapolation) for A_1 nonet predictions as for the B. This is qualitatively consistent with the Kislinger model to be discussed soon and table 12 takes this definition for its theoretical predictions

The remaining rather pauce data on A_1 and B nonet production is summarized in tables 11 and 12 The h data is discredited [8], quite interesting, however, is the $\pi^+n \to D^0p$ data [66] shown in the form of $d\sigma/dt$ in fig 10 The unknown mixing and branching ratio of the D, plus the low energy of the data, precludes unambiguous conclusions, we can, however, be satisfied with the agreement between theory and experiment for the pure octet assignment for the D

Table 13 summarizes our predictions, giving values for the expected cross sections for some $L = 1$ production reactions at 15 GeV/c. $d\sigma/dt$ curves were presented in ref. [3] and are not repeated here. Actually, we should admit that a different and perhaps

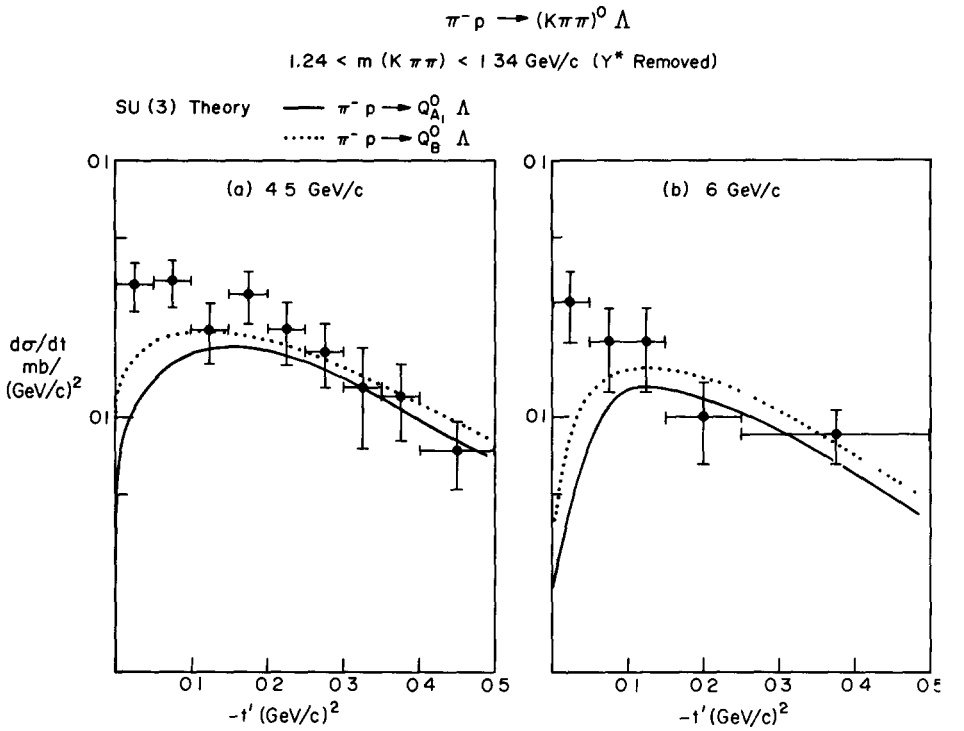

Fig. 9 Comparison of $\pi^- p \rightarrow (K\pi\pi)^0 \Lambda$ data from ref. [26] for the mass-cut 1 24 < $m(K\pi\pi)$ < 1.34 GeV/c with the crossed Y*(1385) bands removed The normalization is simply from the events per microbarn at each momentum corrected for unobserved $K\pi\pi$ charge states. The theoretical curves correspond to the two expected Q mesons, Q_{A_1} and Q_B. As decribed in subsect 4.2, both curves come from halving the value of the Q spin-flip part of the pole extrapolation formulae. This is only justified by SU(3) for Q_B

Table 11
B nonet cross sections *

Reaction	Decay	P_{lab}	$\sigma(\mu b)$ Theory	Expt.	Ref.
$K^- n \rightarrow h^0 \Sigma^-$	$\pi^+\pi^-\pi^0$	2 1	135 (h octet) 53 (h magic-ω)	37 ± 11	[61]
$\pi^+ p \rightarrow h^0 \Delta^{++}$	$\pi^+\pi^-\pi^0$	4	8 (h octet) 23 (h magic-ω)	150	[62]
$K^- n \rightarrow B^- \Lambda$	all	3	31	102 ± 26	[63]
$K^- n \rightarrow B^- \Lambda$	all	4 9	12	29 ± 8	[64]

* Omitting $\pi N \rightarrow BN$ (a compilation of such data may be found in ref. [65]). All theoretical cross sections are calculated by integrating in $0 \leqslant -t' \leqslant 1$ (GeV/c)^2.

Table 12
A_1 nonet cross sections *

Reaction	Decay	P_{lab}	$\sigma(\mu b)$ Theory	Expt	Ref
$\pi^+n \to D^0p$	$\pi_N(980)^{\mp}\pi^{\pm}$	2 7	52 **	44 ± 8	[66]
$\pi^-p \to D^0n$	$K^{\pm}K^0\pi^{\mp}$	2 5 → 2 63	unknown	7 ± 2	[67]
$\pi^-p \to D^0n$	$K^{\pm}K^0\pi^{\mp}$	2 9 → 3 3	$D \to K\bar{K}\pi$ branching ratio	10 ± 4	[67]
$\pi^-p \to D^0n$	$K^{\pm}K^0\pi^{\mp}$	3 8 → 4 2		17 ± 5	[67]
$\pi^+p \to D^0\Delta^{++}$	$\pi^+\pi^-\eta$	8	7 **	25 ± 8	[68]
$K^-p \to D^0\Lambda$	$\pi_N(980)^{\mp}\pi^{\pm}$	5 5	1 5 **	< 6	[69]
$\pi^-p \to Q^0\Lambda$	$(K\pi\pi)^0$	4 5	8	13 5 †	[26]
$\pi^-p \to Q^0\Lambda$	$(K\pi\pi)^0$	6	6 5	8 7 †	[26]

* Omitting diffractive data All theoretical cross sections are calculated by integrating in $0 \leqslant -t' \leqslant 1$ (GeV/c)^2

** Using no decay branching ratio for D and assuming it to be pure octet

† Cross sections from simple mass cuts 1 24 < $m(K\pi\pi)$ < 1 34 (GeV/c)^2, crossed Y* bands removed and $0 \leqslant -t' \leqslant 1$ (GeV/c)^2

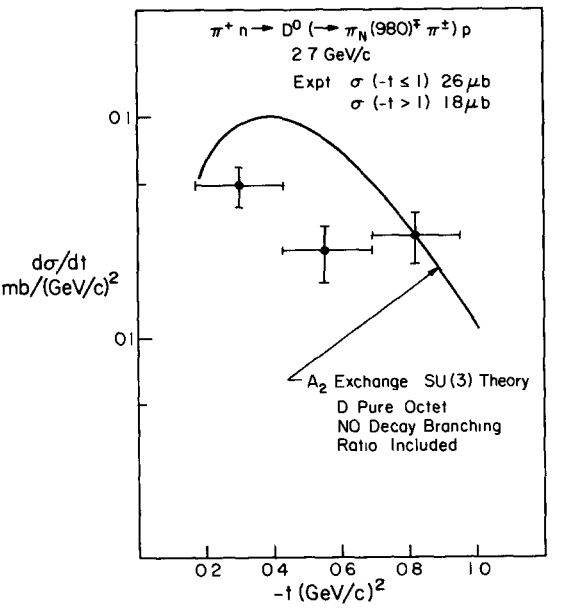

Fig. 10. Comparison of the SU(3) theory discussed in subsect 4 2 with $\pi^+n \to D^0p$ at 2 7 GeV/c from ref [66] We have included no decay branching correction for the theoretical D calculations as the observed $\pi_N(980)^{\mp}\pi^{\pm}$ decay is believed to be dominant We have chosen the pure octet $I = 0$ mixing assignment for the D meson.

Table 13
Predicted natural-parity exchange cross sections at 15 GeV/c

B Nonet	$\sigma(\mu b)$	A_1 Nonet	$\sigma(\mu b)$	A_2 Nonet	$\sigma(\mu b)$
$\pi^- p \to Q_B^0 \Lambda$	1 4	$\pi^- p \to Q_{A_1}^0 \Lambda$	1 15	$\pi^- p \to K^{*0}(1420)\Lambda$	1 1
$\pi^+ p \to Q_B^+ \Sigma^+$	1.65	$\pi^+ p \to Q_{A_1}^0 \Sigma^+$	1 3	$\pi^+ p \to K^{*+}(1420)\Sigma^+$	1.2
$K^- n \to B^- \Lambda$	1 7	$K^- n \to A_1^- \Lambda$	1 4	$K^- n \to A_2^- \Lambda$	1 2
$K^- p \to B^- \Sigma^+$	1.9	$K^- p \to A_1^- \Sigma^+$	1 6	$K^- p \to A_2^- \Sigma^+$	1 4
$K^- p \to h_\omega \Lambda$	1 25	$K^- p \to D_8 \Lambda$	0.25	$K^- p \to f^0 \Lambda$	0 6
$K^- p \to h_\omega \Sigma^0$	0.7	$K^- p \to D_8 \Sigma^0$	0 15	$K^- p \to f^0 \Sigma^0$	0 35
$K^- p \to h_\phi \Lambda$	1 15	$K^- p \to D_1 \Lambda$	0 9	$K^- p \to f' \Lambda$	0 9
$K^- p \to h_\phi \Sigma^0$	0 6	$K^- p \to D_1 \Sigma^0$	0.5	$K^- p \to f' \Sigma^0$	0 5
$K^- p \to Q_B^0 n$	6 15	$K^- p \to Q_{A_1}^0 n$	4 15	$K^- p \to K^*(1420) n$	π
$\pi^- p \to h_\omega n$	4 5	$\pi^- p \to D_8 n$	2 6	$\pi^- p \to f n$	exchange
		$\pi^- p \to D_1 n$	4 0		
$\pi^- p \to B^0 n$	12	$\pi^- p \to A_1^0 n$	2 9	$\pi^- p \to A_2^0 n$	5 1

These come from integrating the SU(3) models in sect 4 for $0 \leq -t' \leq 1$ (GeV/c)^2 at an incident momentum of 15 GeV/c. Isospin invariance may be used to derive other reactions Table 6 will give Δ^{++} and Y* reactions

better definition of our "SU(3) prediction" was given there. Thus, in our earlier paper, we took the *whole* pole extrapolation cross section and multiplied it by experiment divided by theory for $\pi^+ p \to B^+ p$ at 5 and $\pi^- p \to Q_{A_1}^0 \Lambda$ at 4.5 GeV/c. Also some correction was made for EXD violation in these earlier calculations. Here our simpler prescription allows the reader to easily adjust the predictions to account for future knowledge and improvements in the canonical parameters given in subsect. 3.3.

4.3. The peak at small t in B production

We must now come to the feature, first reported [71, 73] at the 1972 Batavia conference which has caused us some considerable pain. We had glossed over the small $-t$ peak in $\pi^- p \to B^- p$ shown in fig. 7 *. This omission seems at first sight rather unforgivable, for the conclusion of the last section was that the B differential cross section was flat and showed no evidence for the non-flip amplitude expected in a naive theory Perhaps the data is showing a small non-flip B coupling, we say small, simply by comparing theory and experiment in fig. 7. However, there is another explanation which requires no B non-flip coupling. Remember that the data [70, 71] plotted in fig. 7 came from a simple $\pi\omega$ mass cut and had no background subtraction. Now a possible background in this reaction is $\pi\omega$ in a $J^P = 1^-$ state.

* A peak at small t in $\pi^+ p \to (\pi\omega)^+ p$ is also seen at 7 GeV/c (ref. [73] and S Flatté, private communication) The effect, in the preliminary data, is less pronounced than in the 9 1 GeV/c $\pi^- p \to B$

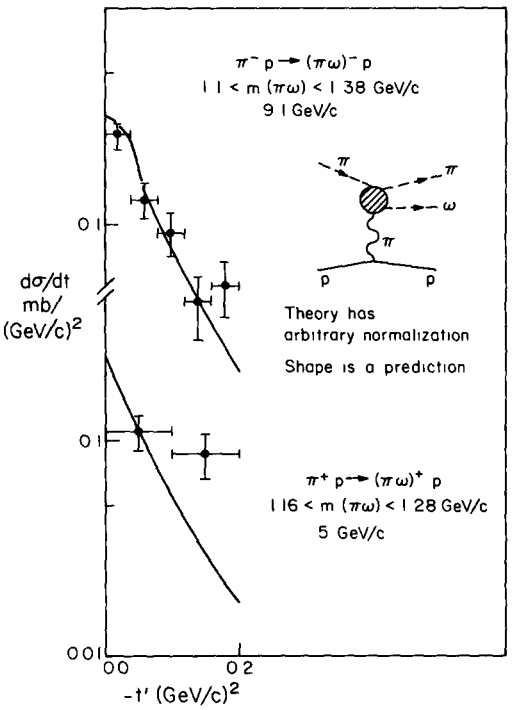

Fig 11 Comparison of $\pi N \to (\pi\omega)N$ data in the B region with the background expected at small t from the π-exchange process $\pi N \to (\rho' \to \pi\omega)N$ See the text (subsect. 4.3) for a specification of the theoretical curves and as to why the normalization of the data in this figure differs from that in fig 7

This, unlike the B, can be produced by π-exchange and is expected to be strongest near $t = 0$. We use the (poor man's absorption) PMA π-exchange model [5] to estimate this background, determining the only unknown parameter (A in e^{At} amplitude t-dependence) from fits to $\pi N \to \rho N$ data. This gives us an unambiguous prediction for the shape of the background t-dependence. Fig. 11 shows this prediction is in striking agreement with experiment Here the theory has been normalized to the data at 9.1 GeV/c This was done because the absolute normalization of the theory has enormous uncertainty as $\pi\pi \to \pi\omega$ scattering is unknown. As an example, we took a $1^- \rho'$ resonance at 1.45 GeV/c with width 300 MeV and the (ridiculous) partial widths $\Gamma_{\pi\pi} = \Gamma_{\pi\omega} = 150$ MeV The curves in fig. 11 come from multiplying this theory by 3. Bearing in mind the numerous uncertainties, this seems O.K (We would be happier however, if experiment had a lower normalization ..)

The discerning reader will have noticed that the normalization of the data in figs. 7 and 11 are different. This occurred because fig, 7 comes from normalizing $d\sigma/dt$ corresponding to a simple mass-cut to the quoted B cross section (the latter coming

from a Breit-Wigner fit to whole mass distribution allowing background and resonance tails, etc.). Fig. 11 was obtained by taking the observed number of events in the mass-cut and normalizing using the event per microbarn equivalent of the experiment. Also note that the theory does not have the expected P^{-2}_{lab} π-exchange behaviour in fig 11 This follows simply from the different mass-cuts used at 5 and 9.1 GeV/c

We should not continue. The correct answer will only come from a careful partial-wave analysis of the original data summary tapes. Note that if one had a nice π^0 detector, $\pi^- p \to (\pi\omega)^0 n$ would be a very favorable place to islolate the π pole. Compared with $\pi^- p \to (\pi\omega)^- p$, π-exchange is *increased* by a factor of 2 and B production reduced by a factor of 2 (calculating the relevant ratio of A_2 to $\omega + A_2$ exchange at 5 GeV/c and small t)

5. Model calculations of natural-parity-exchange meson-resonance cross sections

5.1 Introduction

As we have just seen, it is necessary to account for the apparent suppression of the 1^+ axial vector meson cross sections. This suppression is, in fact, predicted by a model for vector-trajectory Regge couplings recently proposed by Kislinger [7]. In the next subsections, we describe the assumptions of this model and outline some elementary calculations using Kislinger's form for the Regge amplitudes. Our treatment parallels that of Ravndal [74] in a related problem, and we consider both elastic πN scattering and meson-resonance excitation. Since the vector-trajectory couplings in πN elastic scattering are rather well-known (see subsect. 3.3), we can eliminate an unknown overall constant and predict the meson-resonance cross sections in terms of the meson matrix elements of a conserved SU(3) current. To obtain an estimate of these cross sections, it is therefore necessary to have a model for these matrix elements They can be related to virtual-photon amplitudes $M^* \to M + \gamma(q^2)$, and for this we use the FKR relativistic quark model [6] described in subsect 3 5 and appendix B. This model has its deficiencies and ambiguities, but a specific quark model has the virtue of correct SU(3) properties and should give predictions of the right order magnitude.

5.2. Kislinger's model

Kislinger's [7] model is a generalized vector-meson–photon analogy. In the model, the vector-meson Regge-pole couplings are written in terms of a vector operator whose matrix elements are assumed to be proportional to those of the photon *. Kislinger writes the Regge amplitude in the form

$$T(s, t) = \beta(t) s^{\alpha_V(t)-1} \langle l' | R^{\mu}_V | l \rangle \langle b' | R_{V\mu} | b \rangle, \qquad (21)$$

* Kislinger's model may perhaps be made more plausible by recent work (refs [75, 76]) suggesting a connection between the bilocal operators of deep-inelastic ep scattering and reggeon couplings

where, as illustrated in fig. 1, the four momenta of the particles in MN → M*N are l, b, l' and b', respectively. We put $q = l' - l$ whence the standard invariants are $t = q^2$ and $s = (l + b)^2$.

The important ingredient of the model is the assumption that the matrix elements of the vector operator R_V^μ are simply proportional to those of the corresponding conserved SU(3) current J_V^μ. In terms of some universal function $r(t)$, we therefore write

$$\langle k' | R_V^\mu | k \rangle = r(t) \langle k' | J_V^\mu | k \rangle. \tag{22}$$

For the ω and ρ trajectories, we may express the coupling in terms of the familiar electromagnetic current matrix elements.

$$\langle l' | R^\mu_{\substack{(\rho)\\(\omega)}} | l \rangle = r_{\substack{(\rho)\\(\omega)}}(t) \langle l' | J^\mu | l \rangle, \tag{23}$$

where the conservation condition is

$$q^\mu \langle l' | J^\mu | l \rangle = 0. \tag{24}$$

This condition leads to a zero in the non-flip off-diagonal transitions M* → M + $\gamma(q^2)$ for $q^2 = 0$ and so suppresses these amplitudes in resonance M* production This is in qualitative agreement with the data discussed in the previous section. To obtain more quantitative predictions, it is necessary to have some model for the photo-electric meson-resonance matrix elements. This is where we shall turn to the explicit FKR quark model; and in the next subsection, we derive the necessary formulae.

5.3. Formalism

We now outline the kinematics of elastic scattering and meson resonance production:

$$\pi + N \to \pi + N, \tag{25}$$

$$\pi + N \to M^* + N. \tag{26}$$

We evaluate the contribution to the differential cross section resulting from vector-meson Regge-pole exchange, where the Regge amplitude is written as (eqs. (21) and (23))

$$T(s, t) = P(t) s^{\alpha(t)-1} \langle l' | J^\mu | l \rangle \langle b' | J_\mu | b \rangle. \tag{27}$$

$P(t)$ is some universal function, which together with the common baryon-antibaryon vertex, we will eliminate by taking the ratio of reactions (26) and (25) and so predicting (26) in terms of the known differential cross section for (25). Eq. (27) involves the matrix elements of the electromagnetic current and is thus appropriate for ρ^0 and ω^0 Regge contributions. (ω exchange obviously does not contribute to the elastic reaction.) However, note that Kislinger's model has the identical EXD and SU(3) properties to the idyllic world discussed in subsect. 3.2. Thus, it is sufficient to consider just the ρ^0 and ω exchange that are elementarily related to electromagnetic cur-

rent matrix elements. Application of tables 3–5 will then give *all* other vector/tensor exchange processes.

In both cases (i e., reactions (25) and (26)), the matrix element at the nucleon vertex is just the electromagnetic form factor, and, therefore, normalizing our spinors by $\bar{u}u = 2\,m_N$ where $b^2 = b'^2 = m_N^2$, we have

$$\langle b'|J_\mu|b\rangle = \bar{u}(b')\,\Gamma_\mu(t)\,u(b), \tag{28}$$

where $\Gamma_\mu(t) = A(t)\gamma_\mu + B(t)\,(b + b')_\mu$ and $A(t)$, $B(t)$ are just linear combinations of the usual nucleon form factors $G_E(t)$, $G_M(t)$ which need not concern us here.

Now we can write in the high-energy limit

$$\mathrm{d}\sigma/\mathrm{d}t = \frac{1}{16\,\pi s^2}\sum{}' |T|^2, \tag{29}$$

where the spin-averaged $\Sigma' |T|^2$ takes the form

$$\sum{}' |T|^2 = P(t)^2\, s^{2\alpha(t)-2}\, M^{\mu\nu}B_{\mu\nu} \tag{30}$$

Here $M^{\mu\nu}$ and $B^{\mu\nu}$ are respectively meson and baryon tensors

$$M_{\mu\nu} = \langle l'|J_\mu|l\rangle\langle l|J_\nu|l'\rangle, \qquad B_{\mu\nu} = \langle b'|J_\mu|b\rangle\langle b|J_\nu|b'\rangle. \tag{31}$$

Taking the spin-average gives

$$B_{\mu\nu} = \tfrac{1}{2}\,\mathrm{Tr}[(\not{b}' + m_N)\,\Gamma_\mu(t)\,(\not{b} + m_N)\,\Gamma_\nu(t)], \tag{32}$$

where since $q^\mu M_{\mu\nu} = 0$, we may replace b'_μ by b_μ in Γ_μ and so obtain

$$\begin{aligned} B^{\mathrm{eff}}_{\mu\nu} &= \alpha b_\mu b_\nu + \beta g_{\mu\nu}, \\ \alpha &= 4[A^2 + 4m_N AB + B^2(4m_N{}^2 - q^2)], \\ \beta &= q^2 A^2. \end{aligned} \tag{33}$$

Now we must turn to the meson vertex $M_{\mu\nu}$ where we treat the two reactions (25) and (26) separately. In the (simple) elastic scattering (25) we get

$$\langle l'|J_\mu|l\rangle = (l + l')_\mu\, f_\pi(t) \tag{34}$$

where $f_\pi(t)$ is the pion form factor. This leads to the expression

$$\mathrm{d}\sigma/\mathrm{d}t\ (\mathrm{elastic}) = \frac{P(t)^2}{4\pi}\, s^{2\alpha(t)-2}\,\tfrac{1}{4}\,\alpha\,|f_\pi(t)|^2, \tag{35}$$

where one should distinguish α of eq. (33) from trajectory $\alpha(t)$.

Secondly, take the resonance production reaction (26). We can analyze the meson $M_{\mu\nu}$ (summed over the unobserved M* helicities) in a manner familiar from inclusive electroproduction processes. With an ingenious normalization put

$$\begin{aligned} M_{\mu\nu} &= [l_\mu - (l\cdot q)q_\mu/q^2]\,[l_\nu - (l\cdot q)q_\nu/q^2]\,2W_2(q^2)/m \\ &\quad + 2\,m(-g_{\mu\nu} + q_\mu q_\nu/q^2)\,W_1(q^2). \end{aligned} \tag{36}$$

W_1 and W_2 can be calculated in terms of the amplitudes $F_{0,\pm}$ introduced in subsect. 3.5, namely,

$$W_1(q^2) = \frac{m^{*2}}{m}\,[|F_+|^2 + |F_-|^2], \tag{37}$$

$$W_2(q^2) = 2\,m(-q^2/Q^{*2})\,[(-q^2/Q^{*2})\,|F_0|^2 + \tfrac{1}{2}\,(|F_+|^2 + |F_-|^2)],$$

where, as usual,

$$Q^{*2} = \frac{[(m^* + m)^2 - q^2]\,[(m^* - m)^2 - q^2]}{4\,m^{*2}}\,. \tag{38}$$

Taking the high-energy limit, we find

$$\mathrm{d}\sigma/\mathrm{d}t = \frac{P(t)^2}{4\pi}\,s^{2\alpha(t)-2}\,\tfrac{1}{4}\alpha\,[-q^2/Q^{*2}]$$

$$\times\,\{(-q^2/Q^{*2})\,|F_0|^2 + \tfrac{1}{2}\,(|F_+|^2 + |F_-|^2)\} \tag{39}$$

We now take the ratio of (39) and (35) to eliminate α and the unknown $P^2(t)$ This gives

$$\frac{\mathrm{d}\sigma^{V^0}}{\mathrm{d}t}(\pi N \to M^* N) \Big/ \frac{\mathrm{d}\sigma^{V^0}}{\mathrm{d}t}(\pi N \to \pi N) = \frac{\left(\dfrac{-q^2}{Q^{*2}}\right)\left[\left(\dfrac{-q^2}{Q^{*2}}\right)|F_0|^2 + \tfrac{1}{2}\,(|F_+|^2 + |F_-|^2)\right]}{|f_\pi(q^2)|^2}\,. \tag{40}$$

This equation summarizes the content of Kislinger's model for our processes. The amplitudes $F_{0,\pm}$ are obtained from table 9 and some cunning is needed while inserting the correct SU(3) and signature factors from tables 3 to 5 Further, we should note that, as discussed in appendix B, the FKR model has trouble in predicting the q^2 dependence of the $F_{0,\pm}$ amplitudes. So we shall use eq. (40) only to obtain the leading behaviour as $t \to 0$. The t-dependence will be put in *via* the canonical parameterization of subsect. 3.3

5.4 $\pi^+ n \to \omega^0 p$

Before using the formula (40) for speculative estimation of 1^+ cross sections, we first note that we can subject the Kislinger model to a simple test without any additional quark model assumptions. Thus, the model relates the ρ exchange parts of reaction $\pi^+ n \to \omega^0 p$ and $\pi^- p \to \pi^0 n$ to the radiative width of the ω meson. Namely, manipulation of eq. (40) gives

$$\left.\frac{\mathrm{d}\sigma/\mathrm{d}t(\pi^+ n \to \omega^0 p)}{\mathrm{d}\sigma/\mathrm{d}t(\pi^- p \to \pi^0 n)}\right|_{\substack{\rho \\ \text{exchange}}} = \frac{3\pi\,|t|\,\Gamma(\omega \to \pi\gamma)}{e^2\;\;Q^{*3}} \approx 1.7\,|t|. \tag{41}$$

This is perhaps an unreliable prediction as simple Regge theory is a poor approximation to the natural-parity part of $\pi^+ n \to \omega^0 p$. However, let us use our EXD/SU(3)/

factorization folklore to convert eq. (41) into a relation between $K^-p \to K^{-*}p$ and $K^-p \to \bar{K}^0 n$; both of which are dominantly overall spin-flip amplitudes and nicely described by Regge poles.
This gives

$$K^-p \to K^{*-}p \Big|_{\substack{p\bar{p} \text{ non-flip} \\ \text{natural-parity} \\ \text{exchange}}} = 0.66\, K^-p \to \bar{K}^0 n \Big|_{p\bar{n} \text{ spin-flip}} \tag{42}$$

Around 10 GeV/c, this reads [22, 77]

$$\approx 100\ \mu b = 0.66 \text{ of } \approx 50\ \mu b; \tag{43}$$

on estimating the percentage, the dominant terms are of the quoted cross sections. We deduce that Kislinger's model underestimates the K* cross sections by a factor of 3 to 4 in cross section.

This is shown in fig. 12 where we have used eq. (42) for the relative couplings but included subdominant terms using the canonical folklore described in sect. 3. Note how excellently the shape of $K^-p \to K^{*-}p$ is reproduced, this indicates the excellence of the Regge-pole approximation. Shown is not only the Kislinger predictions (41)

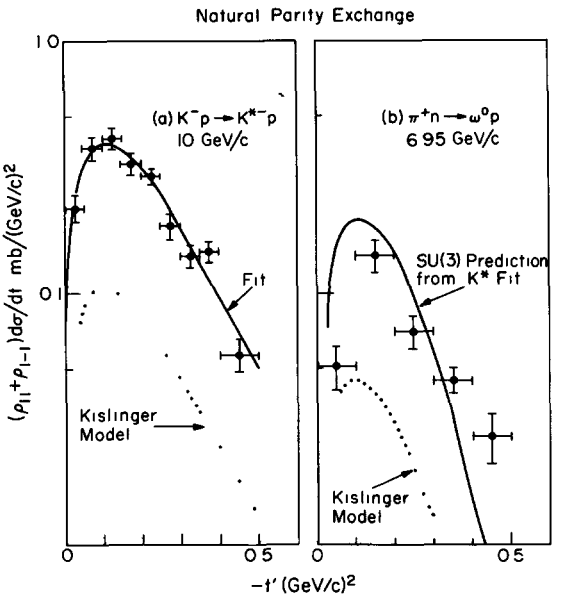

Fig 12 Comparison of the predictions (dotted curves) of the Kislinger model – Eqs (41) and (42) in subsect 5 4 – with experimental data on $K^-p \to K^{*-}p$ (ref [77]) and $\pi^+n \to \omega^0 p$ (ref [78] In each case, the decay density matrix elements of the vector particle have been used to isolate natural-parity exchange The solid curves come from multiplying this prediction by 3 8. SU(3) relates the curves in (a) and (b) as described in subsect. 3.2.

and (42) but the eyeball fit to the K* data gotten by multiplying the Kislinger predictions by 3.8 (in cross section). The deviation of the latter from 1 is then our best measure of the model's reliability.

5.5. Predictions for production of $L = 1$ and $L = 2$ quark states

We now turn to the Kislinger + FKR quark-model predictions (upon every sin is another sin...). To employ it, we use the expression (40) at $t = 0$ and so find the ratio of ρ exchange $\pi^- p \to A_1{}^0 n$, $\pi^- p \to A_2{}^0 n$, $\pi^- p \to h_\omega n$ to $\pi^- p \to \pi^0 n$. This gives us an estimate of PM* → V, T couplings to be used together with the parameters of subsects. 3.2–3 to predict all the cross sections for the production of the 1^+ and 2^+ nonets.

The results are shown in fig. 13 and table 14. They are even more disappointing than ω production foretold – being, in each case, about a factor of 10 too small in cross section. In spite of this, the predicted $d\sigma/dt$ shapes are good and the ratio of B $A_1 . A_2$ production is similar to that in the SU(3) spin-flip pole extrapolation

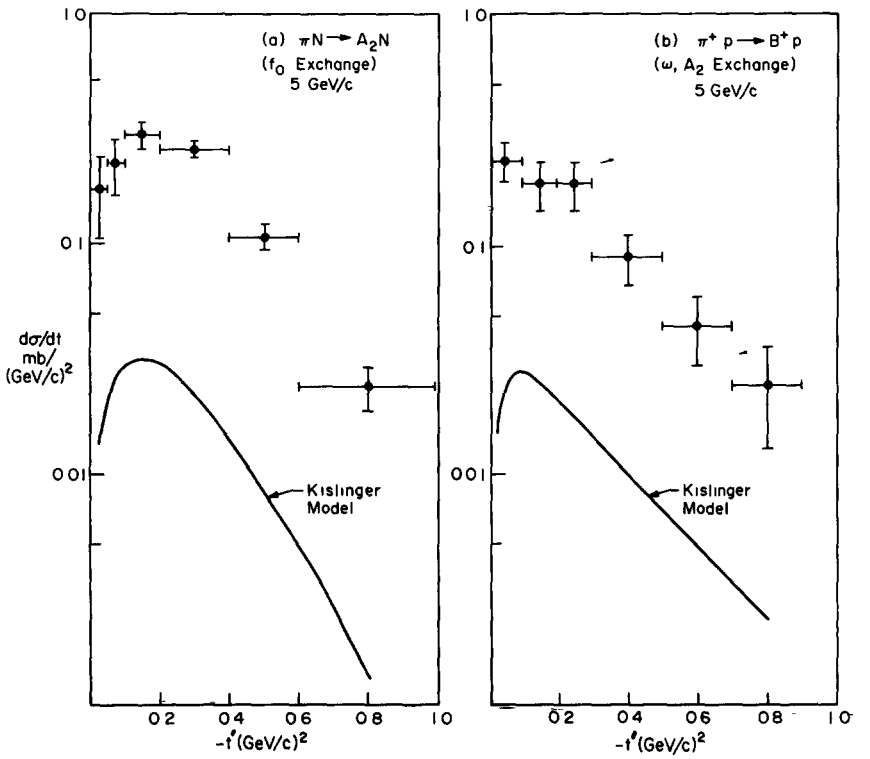

Fig. 13. Comparison of the Kislinger model described in subsect 5 5 with data on $\pi N \to A_2 N$ (ref [51], see fig. 5) and $\pi^+ p \to B^+ p$ (ref. [70], see fig 7)

Table 14
Resonance cross section in μb at 5 GeV/c

Reaction	Expt.	Kislinger Model	*Ad hoc* spin-flip model
$\pi^+p \to B^+p$	92 ± 16 (ref. [70])	10	80 *
$\pi^-p \to A_1{}^0n$	?	1.5	13 5
$\pi N \to A_2N$ ($I = 0$)	127 ± 23 (ref. [51])	12	127
$\pi^+p \to A_3{}^+p$ (f_0 exchange)	?	1.5	
$\pi^+p \to \rho'{}^+p$ (ω, A_2 exchange)	?	0 15	
$\pi^+p \to A_1{}^{*+}p$ (ω, A_2 exchange)	?	0 73	
$\pi^-p \to g^0n$ (A_2 exchange)	?	0.6	

* *Not* a prediction but the defining normalization of all the 1^+ SU(3) predictions discussed in subsect 4 2

model. This adds confidence perhaps to the use of the latter for the prediction of A_1 nonet cross sections.

One curiosity is that, as one might expect from vector dominance, the Kislinger model for $\pi^+n \to \omega^0p$ only deviates from the pole extrapolation model by about a factor of 2 in cross sections. The pole model lies between the dotted and solid curves on fig. 12 and comes from the usual estimate of the $\omega \to \pi\rho$ couplings by assuming this (virtual) state dominates the $\omega \to 3\pi$ decay. However, the similar $A_2 \to \pi\rho$ pole model lies, as shown in table 14, a factor of 10 above the Kislinger model. The failure of the vector dominance model in this case suggests that one might be able to reformulate the Kislinger model to agree better with vector dominance and hence with the data.

Thus, we conclude that the Kislinger model only gives a qualitative description of the data. It could be interesting to subject it to further qualitative tests comparing the πN decay angular distribution observed in $\pi^+p \to \pi^0(\pi^+p)$ (and described by Regge ρ exchange illustrated in fig. 14) with that observed in photoproduction $\gamma N \to \pi N$.

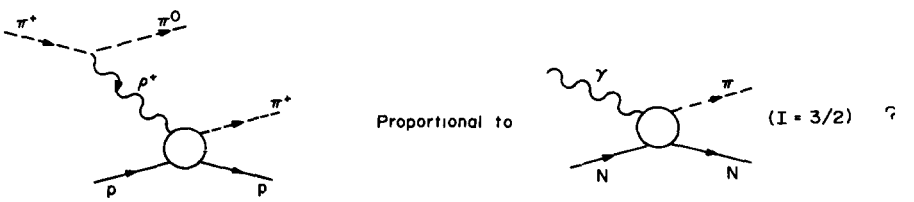

Fig 14 An untested prediction of the Kislinger model discussed in subsect 5.5.

6. Estimation of unnatural-parity-exchange cross sections

We complete our discussion of the production mechanisms of meson resonances by considering the unnatural-parity-exchange component. To be exact, we ignore π-exchange processes, which have large cross sections and are well understood [3, 5], and treat only B and approximately EXD K – Q_B exchange reactions. It turns out that the latter are quite big around 5 GeV/c and often dominate the (suppressed) V–T exchange contributions.

6 1. $\phi_N(1680)$ production

As described in ref. [3], the reaction $\pi^+n \to \phi_N(1680)p$ provides a particularly clean test of the ideas expounded in subsect 3.4 As the 3^- and 1^- nonets have the same charge conjugation and (presumably) the same $I = 0$ mixing, eq. (16) reads

$$\pi^+n \to \phi_N(1680)p \Big|_{\text{B-exchange}} = \pi^+n \to \omega^0 p \Big|_{\text{B-exchange}} \times \frac{\pi^+n \to g^0 p}{\pi^+n \to \rho^0 p}\Bigg|_{\pi\text{-exchange}}, \tag{44}$$

where $\phi_N(1680)$ is the ω-like $I = 0$ magic mixed member of the 3^- nonet. Now the π-exchange ρ and g production reactions have essentially the same t-dependence controlled by our old friend, the pion pole Thus (44) predicts, in agreement with the data shown in fig. 15, that $\phi_N(1680)$ [79] and ω production [78] should have the same t-dependence The relative magnitude is just the ratio of the observed cross sections for g [81] and ρ [80] production. Correcting for non-zero t_{min} suppressing the g production, we get from (44) at 6.95 GeV/c

$$U_{\phi_N}[\pi^+n \to \phi_N(1680)p] = 0.4\,(U_\omega[\pi^+n \to \omega^0 p]) \tag{45}$$

where U_ω, U_{ϕ_N} are respectively the fractions of unnatural-parity (B) exchange in ω and ϕ_N production. Putting in $U_\omega \approx 0.5$, $\sigma(\pi^+n \to \omega^0 p) = 86.4 \pm 12.8$ μb [78], gives 17 μb for the unnatural-parity contribution to ϕ_N production at 6.95 GeV/c. This is nicely consistent with the measured ϕ_N cross section of 33 μb for the dominant (?) $\pi^+\pi^-\pi^0$ decay [79]. This suggests $U_{\phi_N} \approx U_\omega = 0.5$ and so we mark the curve 0 4 ($\pi^+n \to \omega^0 p$) on the plotted ϕ_N data in fig. 15. We predicted the ϕ_N natural-parity exchange * in the last section, but the values are too unreliable to confirm or deny $U_{\phi_N} \approx 0\,5$.

Note that we immediately predict a comparable cross section (i.e. ≈ 30 μb) for $\pi^+p \to \phi_N(1680)\Delta^{++}$. ($\pi^+p \to \omega^0\Delta^{++}$ is bigger than $\pi^-p \to \omega^0 n$, see fig. 3, but the $\phi_N\Delta^{++}$ reaction is suppressed by t_{min})

* Actually the data discussed in subsect 6 3 suggests $U_{\phi_N} \approx 1$ – which is also consistent – if less wondrously – with our estimates above

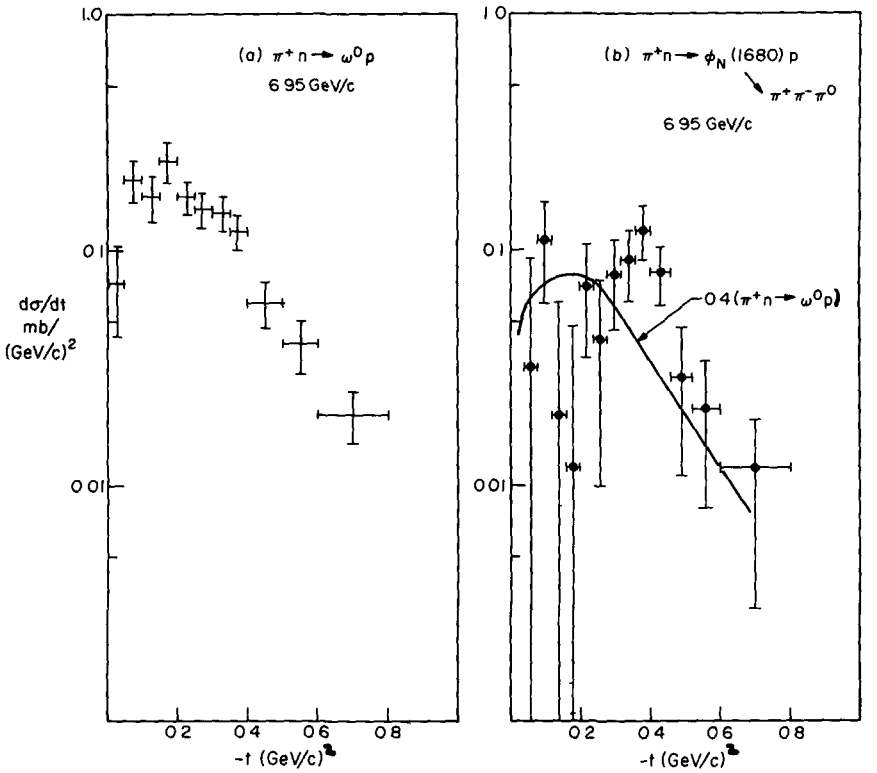

Fig. 15. Comparison of (a) $\pi^+ n \to \omega^0 p$ (ref. [78]) and (b) $\pi^+ n \to \phi_N(1680)p$ (ref [79]) at 6.95 GeV/c discussed in subsect 6.1 The solid curve in (b) is 0 4 times an eyeball fit to the data in (a).

Also we can use the analogue of (44) to predict other $L = 2$ quark state cross sections. In particular, the $I = 0$ member of the $J^{PC} = 1^{--}$ nonet will be produced by B exchange and decay into $\pi^+\pi^-\pi^0$ This cross section will be suppressed by the small $\pi\pi$ coupling of the $I = 1$ member of this nonet [82] (identifying the latter with the ρ') to which coupling, the cross section will by (17) be proportional. However, in view of the mass and mixing uncertainties, we will not pursue these speculations

6.2 $\pi_N(980)$ production

The $\pi_N(980)$ cannot be produced in meson-baryon collisions by either V, T or π-exchange; it can be produced by B exchange in $\pi N \to \pi_N(N, \Delta)$ and $K - Q_B$ exchange in $KN \to \pi_N Y$ Eq. (16) provides a direct estimate of these cross sections in terms of the ratio

$$R = \frac{\sigma(\pi^- p \to \epsilon^0 n)}{\sigma(\pi^- p \to \rho^0 n)} = \frac{2\,\Gamma(\epsilon)}{9\,\Gamma(\rho)} \approx 0.5, \tag{45}$$

which is expressed above as the ratio of the couplings squared at the π pole. These we have evaluated cavalierly to give $R \approx \frac{1}{2}$. The uncertainties in the width, mixing and even assignment to the 0^+ nonet of the ϵ precludes accurate determination of R.

If U denotes "unnatural-parity part", we predict

$$\begin{aligned}
&\pi^- p \to \pi_N{}^0 n = \tfrac{1}{2}\, U(\pi^+ n \to \omega^0 p),\\
&\pi^+ p \to \pi_N{}^0 \Delta^{++} = \tfrac{1}{2}\, U(\pi^+ p \to \omega^0 \Delta^{++}),\\
&K^- p \to \pi_N{}^0 \Sigma^0 = 0,\\
&\tfrac{1}{2}\,(K^- n \to \pi_N{}^- \Lambda) = K^- p \to \pi_N{}^0 \Lambda = \tfrac{1}{2}\, U(K^- p \to \omega \Lambda),\\
&K^- p \to \pi_N{}^- Y^{*+} = \tfrac{1}{2}\, U(K^- p \to \rho^- Y^{*+}).
\end{aligned} \tag{46}$$

The values of the cross sections on the right-hand side are recorded in table 7 and after a small accounting for the t_{min} suppression (this is at worst a factor of 0.75 at 5 GeV/c) directly give the (unknown) $\pi_N(980)$ cross sections. We interpolate table 7 to the desired energies using a P_{lab}^{-2} behavior for B exchange * and P_{lab}^{-3} for strangeness exchange. The results are recorded in table 15 where the agreement between theory and experiment is spotty; theory clearly overestimates the cross sections at the lower momenta. At the higher momenta, there is encouraging agreement. We must await better data on both the left and right sides of (46) to really judge the validity of these relations.

Table 15
$\pi_N(980) \to \pi^- \eta$ cross sections

Reaction	P_{lab}(GeV/c)	$\sigma(\mu b)$		Ref.
		Theory	Expt.	
$\pi^- p \to \pi_N{}^- p$	3 2, 4 12	80	8 ± 4	[84]
$\pi^- p \to \pi_N{}^- p$	5	40		
$\pi^+ p \to \pi_N{}^0 \Delta^{++}$	5	100		
$K^- n \to \pi_N{}^- \Lambda$	2 11, 2.65	unreliable	< 13	[85]
$K^- n \to \pi_N{}^- \Lambda$	4 48	13	15 ± 3	[86]
$K^- p \to \pi_N{}^- Y^{*+}$	3 9, 4.6, 5	13	2.4 ± 1	[87]
$K^- p \to \pi_N{}^- Y^{*+}$	4.1	14	< 6	[69]
$K^- p \to \pi_N{}^- Y^{*+}$	5.5	7	9 ± 3	[69]

* Ref. [83] concludes that the (integrated) unnatural-parity (B-exchange) component of $\pi^+ n \to \omega^0 p$ has an effective intercept in the range 0 to −0.3.

6.3. Production of the 2^+ nonet by unnatural-parity exchange

We can similarly estimate the unnatural-parity contribution of 2^+ nonet production in terms of the ratio

$$R = \frac{\sigma(\pi^- p \to f^0 n)}{\sigma(\pi^- p \to \rho^0 n)} \approx 1.37, \tag{47}$$

which we take from experimental data [88] at 15 GeV/c where t_{min} effects are small. We then get

$$\begin{aligned} &U(\pi^+ n \to A_2{}^0 p) = 1.37\, U(\pi^+ n \to \omega^0 p), \\ &U(\pi^+ p \to A_2{}^0 \Delta^{++}) = 1.37\, U(\pi^+ p \to \omega^0 \Delta^{++}), \\ &U(KN \to (A_2, f^0, \ldots)\Sigma) = 0, \\ &U(\pi^- p \to K^*(1420)\Lambda) = 1.37\, U(\pi^- p \to K^*(890)\Lambda), \end{aligned} \tag{48}$$

and a host of similar relations.

At 5 GeV/c, the experimental [34] cross section for $\pi^+ n \to A_2{}^0 p$ is 190 ± 40 μb Using the work in sect 4, we find the ρ-exchange contribution is but 12 μb. You may argue that this is unreliable for Regge-pole theory is known to be a disaster for the natural-parity part of the basic reaction $\pi^+ n \to \omega^0 p$. However, fig. 12 does show that our SU(3) estimate for $\pi^+ n \to \omega^0 p$, although predicting an unobserved WSNZ (wrong-signature nonsense zero) at $t = -0.6$ (GeV/c)^2, has the right magnitude for small t. Consequently, it underestimates the cross-section by (only) a factor of 2 to 3. We assume this is our error in the A_2 cross section estimate by ρ exchange. Meanwhile, (48) predicts that the B-exchange contribution is 140 μb – in pleasing agreement with experiment and indicating that unnatural-parity exchange is 5 to 10 times bigger than natural-parity exchange at this energy *. As the same ratio in $\pi^+ n \to \omega^0 p$ is around 1 (see, for instance, refs. [34, 35, 78]), it follows that unnatural-parity exchange is, relative to V, T exchange, more strongly coupled to the 2^+ than the 1^- states. Fig. 16 indicates that a similar situation is present in $\pi^+ p \to A_2{}^0 \Delta^{++}$. This figure also confirms that we are predicting the right t-dependence for such processes. Another experimental confirmation can be found in 10 GeV/c $K^- p$ scattering [77], where the ratio π + B exchange/ω + f^0 exchange is found to be larger for $K^- p \to K^{*-}(1420)p$ than for $K^- p \to K^{*-}(890)p$. SU(3), of course, relates this observation to our previous predictions.

We cannot resist commenting that we have previously [16] pointed out that the natural-parity exchange (A_2) pollution of $\pi^+ p \to \rho^0 \Delta^{++}$ is very small at $-t \approx O(m^2_\pi)$ and so this reaction is the best for studying $\pi\pi$ scattering. The above discussion shows that the situation is even better for $\pi^+ p \to f^0 \Delta^{++}$ and as shown in fig 17, at P_{lab} =

* One cannot meaningfully use the $A_2{}^0$ d m e.'s quoted in ref. [34] to estimate the amount of unnatural-parity exchange as the $A_2{}^+$ d.m e.'s in the same reference do not agree with those of ref. [51]

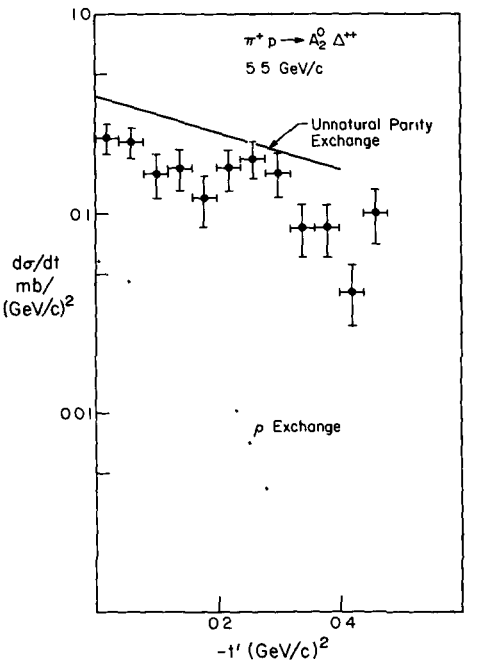

Fig 16 Comparison of experimental data on $\pi^+ p \to A_2^0 \Delta^{++}$ at 5 5 GeV/c from ref [89] with the natural-parity (ρ) exchange contribution calculated as in subsect. 4 1 and the unnatural-parity (B) exchange contribution calculated from eq (48) in subsect 6 3

50 GeV/c (the high momentum makes t_{min} small), the negligible background makes studies of $\pi\pi$ scattering above 1 GeV/c $\pi\pi$ mass very clean [93].

One can predict the unnatural-parity component of the multitude of hypercharge exchange 2^+ reactions (see table 10). However, natural-parity exchange is now no longer represented by sickly spin-flip ρ and A_2, but rather by healthy K*(890, 1420) exchange. Correspondingly, unnatural-parity exchange, although bigger by around a factor of 2, no longer dominates over natural-parity exchange. As there is, as yet, no separation of the data into natural- and unnatural-parity components, a clean discussion is impossible. We will take just one example.

The ratio $\pi^- p \to K^*(1420)\Lambda$ to $\pi^- p \to K^*(1420)\Sigma^0$ in table 10 is larger than the simple V-T exchange prediction. This discrepancy is correctly identified with unnatural-parity exchange which is large for the first and roughly zero for the second reaction. Actually at 4.5 GeV/c, ρ_{00} was measured for $\pi^- p \to K^*(1420)\Lambda$ and found to be * $0.63 \pm 0\,09$ for $0 \leqslant -t' \leqslant 0.5$ (GeV/c)^2. This again indicates the importance

* Similar conclusions can be drawn from the density matrix elements for $K^- p \to (f, f')\Lambda$ reported at 3 9 and 4.6 GeV/c (ref [36])

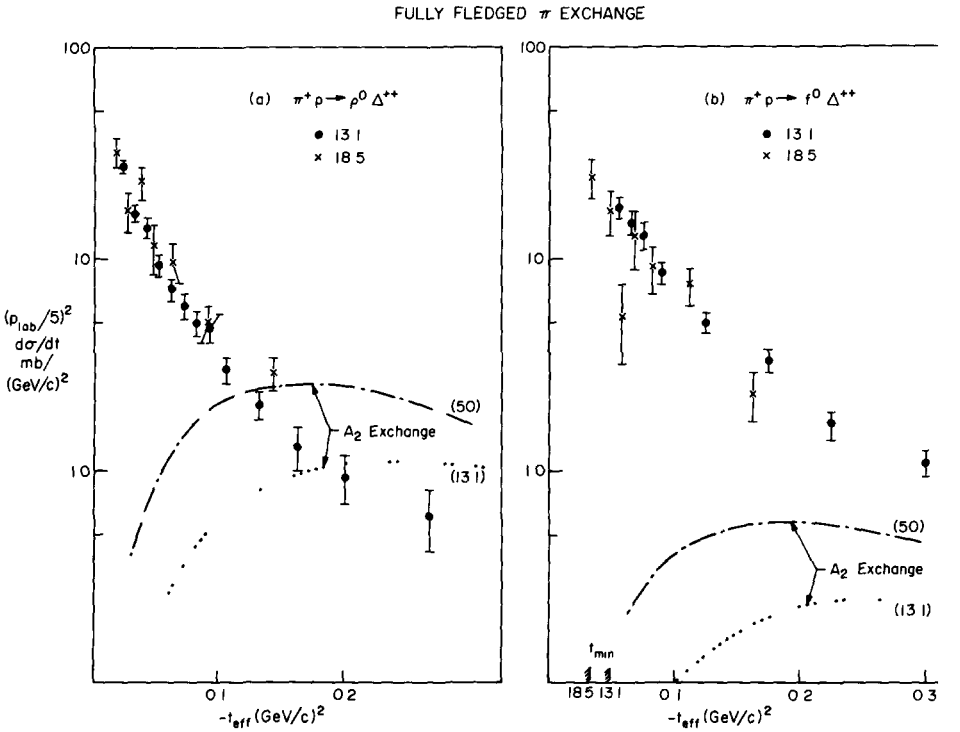

Fig 17. Expected natural-parity exchange (A_2) background in (a) $\pi^+p \to \rho^0\Delta^{++}$ (refs [90, 91]) and (b) $\pi^+p \to f^0\Delta^{++}$ (refs [90, 92]). The theory curves are calculated using the formalism described in subsect. 3.2 and 4 1, and are discussed in subsect 6 3 The deviation of the data in fig. 17b from the universal $P_{lab}^2\, d\sigma/dt$ curve is probably due to different mass cuts used to defin the f^0 in refs [90, 92]. t_{eff} is defined as $t' + t_{min}$ (evaluated with the mean masses of the resonances)

of unnatural-parity exchange for Λ reactions. Table 7 and eq (48) give the curves shown in fig. 18. The predicted unnatural-parity exchange is a factor of 2 to 3 too big. This could be due to many things. For one, our cosmic estimate in table 7 does overestimate the $\pi^-p \to K^*(890)\Lambda$ cross section. Remember this is a moving-phase reaction whose cross section is reduced, for reasons beyond our ken, from the EXD value in table 7. We will not wriggle more but leave this sections as a splendid qualitative success.

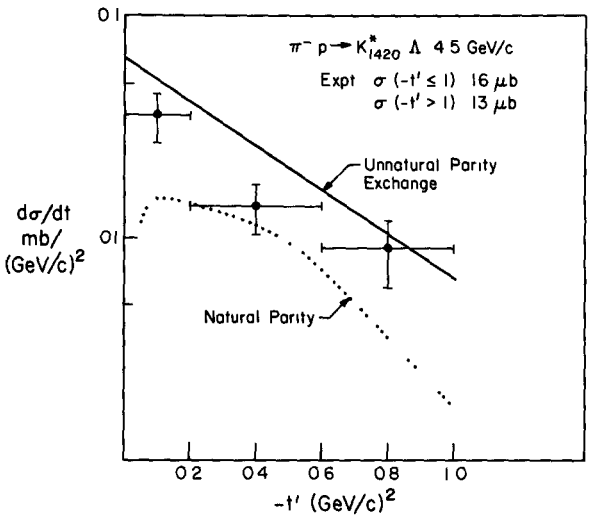

Fig 18 Comparison of experimental data on $\pi^- p \to K^{*0}(1420)\Lambda$ at 4 5 GeV/c (ref [26]) with natural-parity (K*(890) – K*(1420)) exchange contribution calculated as in subsect. 4.1 and the unnatural-parity (K – Q_B) exchange contribution calculated from eq. (48) in subsect. 6 3

7. Photoproduction of meson resonances

One of the lessons of the previous sections was that our poor knowledge of the 1^+ nonets reflected their small hadronic cross sections compared with, say, healthy π-exchange reactions, for instance, $\pi^- p \to \rho^0 n$ and $\pi^+ p \to f^0 \Delta^{++}$ (see fig 17). It is interesting to note that the B and A_1 can be produced by π-exchange in photon induced processes. Their expected cross sections can be estimated reliably by pole extrapolation; failure to observe them with the predicted size would be unambiguous evidence against their existence. As we saw in fig. 7, pole extrapolation for their hadronic production by vector-tensor exchange is a trickier business.

Consider a typical process

$$\gamma + p \to M^{*+} + n \tag{49}$$

where M* is any non-strange I=1 meson resonance. We can calculate the π-exchange Born amplitude (illustrated in fig. 19) as

$$T^{\text{Born}} = e \langle M^* | j_\pi(0) | \gamma \rangle \frac{1}{t - m_\pi^2} \langle N | J_\pi(0) | N \rangle . \tag{50}$$

This can be evaluated at the pion pole in terms of the $\pi N\bar{N}$ coupling G and the $M^{*+} \to \pi^+ \gamma$ radiative width. As described in subsect 3.5, we use the FKR quark model to estimate the latter. The Born cross section given by (50) can be calculated as (taking

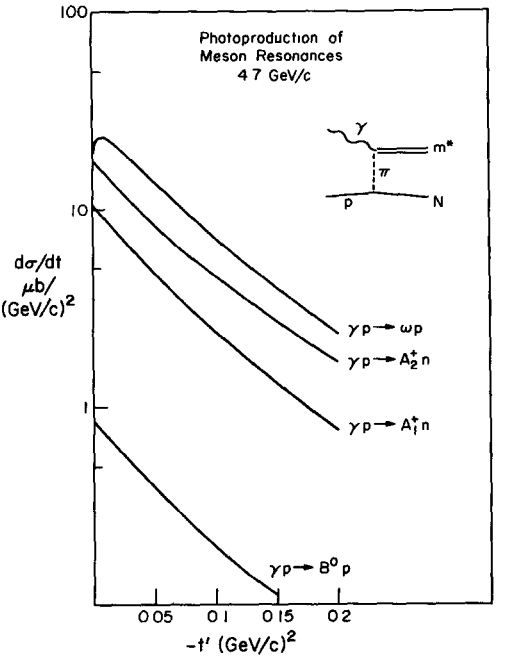

Fig. 19. Production of meson resonances by π-exchange at 4.7 GeV The theoretical curves are discussed in sect 7. As described there, the cross sections quoted in table 16 correspond to half the $d\sigma/dt$ values in the figure

the charged π-exchange reaction (49))

$$d\sigma_{\text{Born}}/dt = 2\,[\pi\alpha G^2/4\pi]\;\frac{1}{(s-m_N^2)^2}\;\frac{|t|}{(t-m_\pi^2)^2} \times 2\,m^{*2}\,(|F_+|^2 + |F_-|^2). \tag{51}$$

The quantities $|F_+|^2 = |F_-|^2$ are gotten by placing $q^2 = 0$ in the formulae of table 9. Using this table plus eq. (51) gives the cross section ratios reported in table 16. As usual one can finesse the argument, and use the pole-coupling values implicit in eq. (51) plus the PMA model [5] for off-shell π-exchange processes. After fitting $\pi N \to \rho N$ (as described in the $\pi N \to (\rho' \to \pi\omega)N$ calculations of subsect. 4.3), this is a parameter-free theory. The results are given in fig. 19.

Note that the FKR model predicts $\Gamma(\omega \to \rho\gamma) = 1.9$ MeV – essentially twice the experimental value. Correspondingly the theoretical $d\sigma/dt$ for $\gamma p \to \omega p$ in fig. 19 is around twice the experimental value. One should perhaps then also halve the predicted $d\sigma/dt$ for A_1, A_2 and B in fig. 19. However, there is no compelling reason as to why the failure of the FKR model is a simple meson independent overall factor.

Table 16
Cross sections for π-exchange in M* photoproduction

Reaction	Cross section (μb) at E_γ = 4 7 GeV *
$\gamma p \to \omega p$	1.25 (theory normalized to this value from ref [94])
$\gamma p \to B^0 p$	0 1
$\gamma p \to A_1^+ n$	0 5
$\gamma p \to A_2^+ n$	0 9

* Cross sections at other energies may be estimated using P_{lab}^{-2} behaviour of π-exchange processes.

Anyhow, we have adopted this simple expedient in table 16 and have renormalized the cross-section estimates by experiment over theory for $\gamma p \to \omega p$ (This is the *unnatural*-parity part of $\gamma p \to \omega p$ extracted [94] using polarized photon data.) Our prediction for $\gamma p \to A_2^+ n$ of 0.9 μb at 4.7 GeV compares satisfactorily with the data $\sigma = (1.2 \pm 0.4)$, $(2.5\ ^{+1\ 5}_{-1\ 0})$, $(0.6 \pm 0\ 3)$ at 4.3 (ref. [95]), 4.7 (ref. [96]), and 5.25 GeV (ref [95]), respectively. There is no report of $\gamma p \to A^+{}_1 n$ as yet * – it would be interesting to look for our $\frac{1}{2}$ μb predicted cross section around 5 GeV. As we have emphasized, non-observation of the A_1 at this level of cross-section would be decisive evidence against its existence.

$\gamma p \to$ "B"p has been reported [96] with a 1 μb cross section around 5 GeV/c. This is much larger than our estimate (which is so small because the π-exchange couples to the "ω part" of $\gamma = \rho + \frac{1}{3}\omega$). A 1 μb cross section is presumably natural-parity exchange (A_2 or Pomeranchuk)

Using the results of table 9, one can also calculate the π-exchange contribution to the production of the $L = 2$ quark states. At low energies, these are suppressed by t_{min} effects, but once this straitjacket is o'ercome, $\gamma p \to \phi_N(1680)p$ is some 10% of $\gamma p \to \omega p$ The other $L = 2$ mesons coupling to the ρ part of the photon have similar cross sections, while those, e.g. $\gamma p \to g^+ n$, that have the misfortune of seeing but the ω-like photon are, as usual, $(\frac{1}{3})^2$ smaller, i.e. around 1% of $\gamma p \to \omega^0 p$.

Finally, we give in fig 20, the PMA predictions for the produced M* resonance density matrix elements. Those for $\gamma p \to \omega p$ are, of course, obscured by the large Pomeranchuk term. The other reactions should, however, be realistic and observable

* We would like to thank Dr G Smadja for many conservations on the experimental difficulties with $\gamma p \to A^+{}_1 n$.

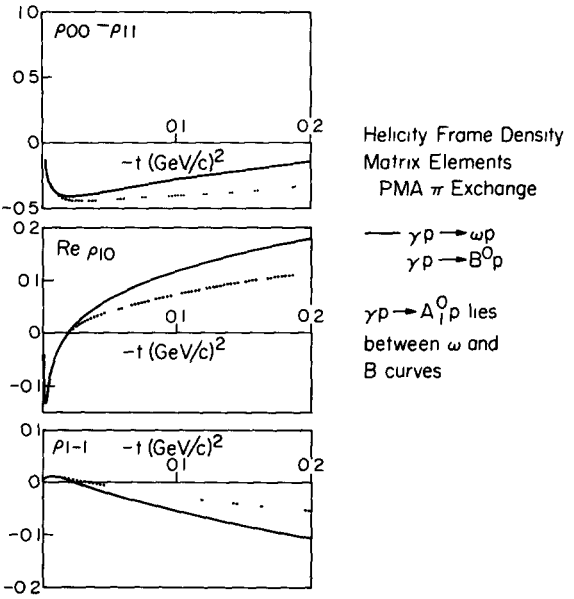

Fig. 20 Predictions of the PMA π-exchange model for the decay density matrix elements for vector mesons photoproduced by π-exchange This figure is discussed in sect. 7

8. Conclusions

We have done battle with the filth and pestilence of experimental data; predicting the essentially unknown cross section in terms of the barely known. We have curdled together many theories (Regge poles, SU(3), factorization, EXD, pole extrapolation, Regge-pole–photon analogy), each of which is only accurate to some factor of 2. Nevertheless, a pleasing picture has emerged.

Firstly, the current poor knowledge of the 1^+ (and similarly of higher – perhaps non-quark) meson states is only temporary. Their predicted cross sections recorded in tables 13 and 16 should be easily within reach of future spectrometer or large bubble-chamber experiments. These mesons can be fruitfully examined in both hadronic and photoproduction non-diffractive processes.

There is a pretty structure in the exchanged quantum numbers around 5 GeV/c, which will clearly repay deeper investigation We find flat cross sections – only half of which lies in $-t < 1$ (GeV/c)^2. We find large unnatural-parity exchange in 0^+, 2^+ and 3^- production – its strength increases relative to natural-parity exchange as we increase the mass of the produced meson and move up the $\rho - A_2$. . trajectory We find natural-parity-exchange cross sections whose non-flip components are greatly suppressed. This can be qualitatively understood in a vector-meson–photon analogy model recently proposed by Kislinger. A quantitative explanation is, however, still lacking.

We found a possible π-exchange peak peeping out at small t in $\pi^- p \to (\pi\omega)^- p$; this suggests that quantitative studies of $\pi\pi \to \pi\omega$ may well be possible in the future.

We wonder what systematics await discovery for forward-baryon and backward-meson resonance formation. We hope our work will stimulate theoretical and experimental study in these fields.

We would like to thank Mark Kislinger and Finn Ravndal for theoretical advice, K.W. Lai and H.A. Gordon for an invaluable DST and Alex Firestone for help in processing it.

One of us (AJGH) does not feel he deserves any credit for the poetic value of this work.

Appendix A. Explicit pole-extrapolation formulae

Here we record the formulae relating the s-channel residues $g_{\mu_3\mu_1}(t)$, introduced in subsect. 3.1, at $t = m_V^2$ to the decay width Γ of $3 \to 1 + V$(V with mass m_V is the (1^-) particle on the exchanged Regge trajectory R in fig. 1).

Specializing at once to the special case of interest $s_1 = 0$, $\mu_1 = 0$, we have, from general principles,

$$g_{\mu_3}(m_V^2) = \sum_{\lambda_3} \sqrt{\frac{\pi\Gamma(2\alpha+1)}{\Gamma(\alpha+\lambda_3+1)\Gamma(\alpha-\lambda_3+1)}}$$

$$\times (m_V/T_{13})^\alpha \exp(\tfrac{1}{2} i\pi\lambda_3)(-1)^{s_3+\lambda_3} \tilde{\gamma}_{\lambda_3} d^{s_3}{}_{\lambda_3\mu_3}(-\chi_3^\infty), \tag{52}$$

where $t = m_V^2$, $\alpha = 1$,

$$T_{13}^2 = [t-(m_1+m_3)^2]\,[t-(m_1-m_3)^2],$$
$$\cos\chi_3^\infty = -[t+m_3^2-m_1^2]/T_{13}, \tag{53}$$
$$\sin\chi_3^\infty = 2m_3 m_V i/T_{13}.$$

Finally, $\tilde{\gamma}_{\lambda_3}$ is the (t-channel) helicity amplitude $\bar{V} \to 1 + \bar{3}$, and is related to the generally more useful $3 \to 1 + V$ amplitude by an irrelevant helicity independent ± 1 sign. The latter amplitude (also denoted $\tilde{\gamma}_{\lambda_3}$) is related to $\Gamma(3 \to 1 + V)$, the width for 3 to decay into 1 + V, by

$$\Gamma(3 \to 1+V) = \sum_{\lambda_3} |\tilde{\gamma}_{\lambda_3}|^2 Q^*/(8\pi(2s_3+1)m_3^2), \tag{54}$$

where Q^* is the momentum of 1 or V for the decay of 3 at rest. Using the observed value for $\Gamma(3 \to 1 + V)$, eq. (54) enables one to determine $\Sigma_{\lambda_3}|\tilde{\gamma}_{\lambda_3}|^2$. If there is only one independent spin amplitude, this is sufficient to determine $g_{\mu_3}(m_V^2)$, up to an irrelevant phase, using (52). Otherwise, one needs a model for spin (λ_3) dependence of the decay amplitude.

For the tensor meson decays, $2^+ \to 0^-1^-$, parity allows only a D-wave decay, (or equivalently, one independent t-channel helicity amplitude), and the decay width is indeed sufficient to determine the s-channel helicity residue g_{μ_3}. For the axial vector meson decays, $1^+ \to 0^-1^-$, the situation is more complicated since both S and D waves are allowed, corresponding to both helicity 1, and helicity 0, decay amplitudes being non-zero. To determine the s-channel g_{μ_3} residues, it is necessary to have a model for the amount of D wave present, since this essentially determines g_{μ_3}. This we shall take from a naive $SU(6)_W$ quark coupling model for the decay. The model predicts that one helicity amplitude for A_1 and B decay is actually zero, this corresponds to the S and D wave amplitudes exactly canceling in one helicity amplitude. Colglazier and Rosner [10, 11] have suggested that this is in disagreement with experiment and, in fact, that the S-wave component in this model may be unreliable. Nevertheless, their analysis showed that the magnitude of the S- and D-wave contributions was actually in reasonable agreement, and that only the relative S-D phase prediction of the $SU(6)_W$ model was violated. As can be seen from eq. (52), the value of g at $t = 0$ essentially depends on the magnitude of the D-wave contribution; so we are content to use the naive $SU(6)_W$ model [97] for the |D|/|S| ratio. The reader is referred to FKR [6] (subsect 3.5, appendix B) or Colglazier and Rosner [10, 11] for the more sophisticated approaches.

In a collinear frame, the $SU(6)_W$ symmetric vertex functions may be constructed in a simple way from quark graphs. The SU(6) wave functions for the $L = 0$ and $L = 1$ mesons are [11]

$$
\begin{aligned}
&M^{(\alpha a)}{}_{(\beta b)} = P^{\alpha}{}_{\beta}\, C_{ab} + V^{\alpha}{}_{\beta}\,(\epsilon\cdot\sigma C)_{ab}, \qquad L = 0,\\
&M_i^{(\alpha a)}{}_{(\beta b)} = B^{\alpha}{}_{\beta}\,\epsilon_i' C_{ab} + \frac{1}{\sqrt{3}} S^{\alpha}{}_{\beta}(\sigma_i C)_{ab}\\
&+ A^{\alpha}{}_{\beta}\frac{1}{\sqrt{2}}\,\epsilon_{ijk}\epsilon'_j\,(\sigma_k C)_{ab} \qquad (55)\\
&+ T^{\alpha}{}_{\beta}\,\epsilon_{ij}\,(\sigma_j C)_{ab}, \qquad L = 1.
\end{aligned}
$$

The symbols P, V, B, S, A and T are the 3 × 3 matrices for the 0^{-+}, 1^{--}, 1^{+-}, 0^{++}, 1^{++}, 2^{++} meson nonets, respectively. The 2 × 2 matrix C in quark spin space is

$$
C = i\sigma_y = \begin{vmatrix} 0 & 1 \\ -1 & 0 \end{vmatrix}. \qquad (56)
$$

The index i represents a polarization vector for one unit of angular momentum, and ϵ_i, ϵ'_i, ϵ_{ij} specify the polarization of the vector, axial-vector and tensor mesons respectively. $SU(6)_W$ invariant vertices are constructed by contracting indices according to the quark graphs (see fig. 21) and insisting that W-spin is conserved in the creation of the $q\bar{q}$ pair. The coupling then has the form

$$
M_z^{+(\gamma c)}{}_{(\alpha a)}\, M^{(\alpha a)}{}_{(\beta b)}\, D_{b\bar{d}}\, M^{(\beta d)}{}_{(\gamma c)} \qquad (57)
$$

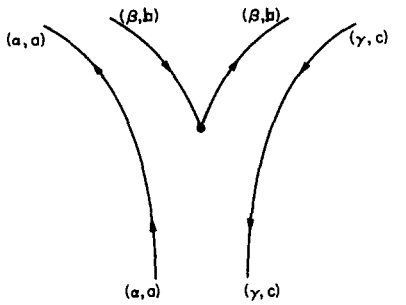

Fig 21 Quark model graph for the 3-meson vertex calculated in appendix A Each quark is represented by a pair of indices (α, a) where α specifies its SU(3) and a its spin state.

The matrix

$$D = \frac{1}{\sqrt{2}}\begin{bmatrix} 0 & 1 \\ 1 & 0 \end{bmatrix} = \frac{1}{\sqrt{2}}\sigma_z C \tag{58}$$

insures that $\bar{q}_b$ and q_d are created in a spin state $S = 1, S_z = 0$, i.e. a state of W-spin zero. This prescription is the natural extension of $SU(6)_W$ from $L = 0$ meson couplings to a coupling involving an $L = 1$ meson. W-spin is still conserved. This symmetry is sometimes called $SU(6)_W \otimes O(2)_{L_z}$.

The predictions are summarized in table 17. To use them, we decompose the predicted helicity amplitudes into S and D partial waves and correct the latter by $(Q^*/Q_0)^2$ where Q_0 is taken as 0.42 GeV/c – an average decay momentum for the $L = 1$ multiplet Table 17 then gives us the necessary ratio of spin states to allow eqs. (52) and (54) to determine $g_{\mu_3}(m_V^2)$ absolutely.

For completeness, we remember that for our pole extrapolation predictions, we need the ratio of, say, $g(\pi A_1 \rho)$ to $g(\pi\pi\rho)$. The latter can be found from eq. (54) using $\Gamma(\rho \to \pi\pi)$ to find directly $\tilde{\gamma}(\rho \to \pi\pi)$ – for as we said, this only differs by an

Table 17
$SU(6)_W \otimes O(2)_{L_z}$ predictions for $L = 1$ meson decays M* → PV

M*	Helicity amplitudes	
	$\tilde{\gamma}_{\lambda=0}$	$\tilde{\gamma}_{\lambda=1}$
$2^{++}(A_2$ nonet)	0 (from parity)	$-1/\sqrt{2}\,\alpha\langle T[V, P]\rangle$
$1^{++}(A_1$ nonet)	0	$-1/\sqrt{2}\,\alpha\langle A[V, P]\rangle$
1^{+-} (B nonet)	$\alpha\langle B\{V, P\}\rangle$	0

Here α is an arbitrary parameter, A, T, V and P are 3 × 3 SU(3) matrices (see text of appendix A), [ ] = commutator, { } = anticommutator and ⟨ ⟩ = trace. The SU(3) isoscalar part of the traces are precisely the numbers given in tables 4 and 5.

irrelevant sign from the explicit case $\tilde{\gamma}(\pi \to \pi\rho)$ for which (54) is written. For the record, we note (54) gives

$$|\tilde{\gamma}(\pi \to \pi\rho)| = 5.35 \qquad \text{for } \Gamma_\rho = 120 \text{ MeV},$$
$$|\tilde{\gamma}(K \to \pi K^*(890)| = 3.2 \qquad \text{for } \Gamma_{K^*} = 50 \text{ MeV}. \tag{59}$$

As usual, these numbers must be multiplied by an appropriate Clebsch-Gordan coefficient to get the coupling for a given charge state.

Appendix B. FKR Quark model for meson-resonance excitation

We review the formalism of ref. [6] used in subsect. 3.5. The mesons are represented as states of a quark-antiquark ($q\bar{q}$) system which is described by the (essentially mass-squared) operator

$$K = 2(P_a^2 + P_b^2) + \tfrac{1}{16}\Omega^2(u_a - u_b)^2;$$

P_a and P_b are the quark and antiquark four-momenta, respectively, and u_a and u_b the corresponding conjugate position variables. The external momentum of the $q\bar{q}$ state may be separated by introducing the total momentum $P = P_a + P_b$ and an internal momentum ζ

$$P_a = \tfrac{1}{2}P - \frac{1}{2\sqrt{2}}\zeta, \qquad P_b = \tfrac{1}{2}P + \frac{1}{2\sqrt{2}}\zeta, \tag{60}$$

with position variables R and z conjugate to P and ζ:

$$u_a = R - \sqrt{2}\,z, \qquad u_b = R + \sqrt{2}\,z. \tag{61}$$

The mass-squared operator becomes

$$K = P^2 - N, \tag{62}$$

where

$$-N = \tfrac{1}{2}\zeta^2 + \tfrac{1}{2}\Omega^2 z^2,$$

N is the true mass-squared operator and depends only on the internal motion, for mesons N has the form of a simple four-dimensional harmonic oscillator, giving eigenvalues spaced by Ω As usual, in harmonic-oscillator problems, it is convenient to introduce creation and annihilation operators for the internal oscillator excitations

$$c^+ = \sqrt{\frac{1}{2\Omega}}\zeta + i\sqrt{\frac{\Omega}{2}}\,z, \qquad c = \sqrt{\frac{1}{2\Omega}}\zeta - i\sqrt{\frac{\Omega}{2}}\,z. \tag{63}$$

These satisfy the communication relation

$$[c_\mu, c^+_\nu] = -g_{\mu\nu}. \tag{64}$$

Thus, to exclude time-like excited states with negative norm, the physical assumption is made that in the rest system of the meson, only space-like excitations exist

$$(P\cdot c)|\mathrm{M}^*\rangle = 0. \tag{65}$$

The vector current is obtained by a minimal coupling prescription

$$\not{P}_a \to \not{P}_a - e_a \not{A}, \tag{66}$$

which leads to an interaction δN^V, with a wave of polarization vector e_μ and momentum q_μ, given by

$$\delta N^V = e^\mu J_\mu = e^\mu \, 2 \sum_{\alpha=a}^{b} e_\alpha (\not{P}_\alpha \gamma_\mu \, e^{iq\cdot u_\alpha} + \gamma_\mu e^{iq\cdot u_\alpha} \not{P}_\alpha). \tag{67}$$

If we use symmetrized SU(3) wave functions for the quark a and antiquark b in the meson, treating the antiquark simply as a quark of negative charge, the sum over α may be removed. One calculates only the contribution from the quark a and multiplies by 2 eq. (67) becomes

$$e\cdot J = 4 \, e_a e^{iqu_a} \, (2(P_a\cdot e) - \not{q}\not{e}). \tag{68}$$

We now specialize our results to the frame in which the initial excited meson of momentum l' is at rest and the virtual photon of momentum q is emitted in the positive z-direction. Elementary kinematics in this frame may be summarized as

$$\begin{aligned} &l' = l + q, \quad l'^2 = m^{*2}, \quad l^2 = m^2, \\ &l' = (m^*, \mathbf{0}), \quad l = (E_2, -\boldsymbol{Q}^*), \quad q = (\nu^*, \boldsymbol{Q}^*), \end{aligned} \tag{69}$$

where

$$\begin{aligned} \nu^* &= \frac{m^{*2} - m^2 + q^2}{2m^*}, \\ Q^{*2} &= \frac{1}{4m^{*2}} [(m^* + m)^2 - q^2] \; [(m^* - m)^2 - q^2], \\ g^2 &= \frac{E_2 + m}{2m} = \frac{(m^* + m)^2 - q^2}{4mm^*}. \end{aligned} \tag{70}$$

We can now follow the same procedure, detailed for baryons by FKR, to express the current operator in a form to be evaluated between two-component Pauli spinors. We obtain

$$\begin{aligned} J_\mu e^\mu = {} & 4 \, g^2 \exp \left[\tfrac{1}{2} q^2 \Omega - \sqrt{1/\Omega} \, q\cdot c^+\right] e_a \\ & \times \{[m^* - \tfrac{1}{2}\nu^* - Q^{*2}/2mg^2 - \sqrt{\tfrac{1}{4}\Omega} \, (c_0{}^+ + c_0)] \, e_0 \\ & + \sqrt{\tfrac{1}{4}\Omega} \, (c^+ + c)\cdot e + Q^*\cdot e \, [\tfrac{1}{2} + \nu^*/2mg^2] \\ & + \imath \, \sigma\cdot Q^* \wedge e \, [1 + \nu^*/2mg^2]\} \exp \left[1/\sqrt{\Omega} \, q\cdot c\right], \end{aligned} \tag{71}$$

where one should distinguish the charge e_a of the quark from the polarization vector $(e_0, \boldsymbol{e})$. For transitions to final state mesons in the ground state, the interaction "simplifies" to.

$$J_\mu e^\mu = 4\, G(m^*, q^2)\, e_a \times \{[m^* - \tfrac{1}{2}\nu^* - Q^{*2}/2mg^2]\, e_0 + \sqrt{\tfrac{1}{4}\Omega}\, \boldsymbol{e}\cdot\boldsymbol{c} + \boldsymbol{Q}^*\cdot\boldsymbol{e}\,[\tfrac{1}{2} + \nu^*/2mg^2] + \imath\,\boldsymbol{\sigma}\cdot\boldsymbol{Q}^*\wedge\boldsymbol{e}\,[1 + \nu^*/2mg^2]\}\exp[-\delta\, c_z], \tag{72}$$

where we have placed

$$G(m^*, q^2) = g^2 \exp[q^2/2\Omega], \quad \delta = Q^*/\sqrt{\Omega}. \tag{73}$$

With all this preliminary, it is straightforward to calculate the helicity amplitudes $F_{\pm,0}$.

$$2m^* F_\mu = \langle M|J_\mu|\mathrm{M}^*\rangle, \tag{74}$$

F_0 is given by the matrix element of J_0 and $F_\pm$ by the corresponding spherical components of J_μ,

$$F_\pm = \mp\frac{1}{\sqrt{2}}(F_x \pm iF_y).$$

The results are

$$F_0(q^2) = 4\, G\,\langle \mathrm{M}|e_a\, \tilde{s}\, \mathrm{e}^{-\delta c_z}|\mathrm{M}^*\rangle,$$
$$F_\pm(q^2) = 4\, G\,\langle \mathrm{M}\,|\,e_a\,\{\tilde{t}\,c_\mp + \sigma_\pm\, r\}\,\mathrm{e}^{-\delta c_z}|\mathrm{M}^*\rangle, \tag{75}$$

where

$$\tilde{s} = \frac{1}{8m^{*2}}[4\, mm^* + m^{*2} - m^2 + q^2], \quad \tilde{t} = \sqrt{\Omega}/4m^*, \tag{76}$$
$$r = \frac{\sqrt{2}\, Q^*\,(m+m^*)}{[(m+m^*)^2 - q^2]}.$$

The operators

$$c^\dagger{}_\pm = \mp\frac{1}{\sqrt{2}}(c_x^\dagger \pm iC_y^\dagger),$$

are the creation operators for states of definite z-component of orbital angular momentum. Note that we have defined

$$\sigma_\pm = \tfrac{1}{2}(\sigma_x \pm \imath\sigma_y).$$

With the above formalism, we can now calculate all our meson radiative matrix elements in the way illustrated for baryons in appendix 4 of FKR. The meson wave

functions are written in the usual way, as an example, we give those for the π^+ and ρ^+.

$$|\pi^+\rangle = \frac{1}{\sqrt{2}}(u\bar{d} - \bar{d}u)\frac{1}{\sqrt{2}}(|+\rangle|-\rangle - |-\rangle|+\rangle)|0\rangle$$

$$|\rho^+\rangle = \frac{1}{\sqrt{2}}(u\bar{d} + \bar{d}u)\begin{Bmatrix} |+\rangle|+\rangle \\ 1/\sqrt{2}\,(|+\rangle|-\rangle + |-\rangle|+\rangle) \\ |-\rangle|-\rangle \end{Bmatrix}|0\rangle$$

where u, d (and s) label the three quarks, $|+\rangle$ and $|-\rangle$ are their two spin states and $|0\rangle$ is the ground state of the spatial oscillator. The $L = 1$ and 2 wave functions are constructed similarly and the relevant results are recorded in table 9 and discussed in subsect 3.5 and sects. 5, 7.

Finally, we must admit that a multitude of sins are absorbed in G whose definition must be changed from its naive value (73). The formulae, as derived, imply the degenerate mass formulae

$$m^{*2}(N) = m^2 + N\,\Omega \tag{77}$$

for a multiplet corresponding to N excitations. However, we will use the non-degenerate observed masses in actual calculations. This is not without repercussions, for instance, the current conservation condition

$$\nu^* F_0 = q^* F_z \tag{78}$$

is only satisfied for the degenerate mass spectrum (77). Evaluated with observed masses, (78) is violated and this is particularly disastrous for the light mass π. Similarly the $F_{0,\pm}$ amplitudes in table 9 only give correct threshold behavior (orbital angular momentum state l behaves like Q^{*l}) for the symmetrical value (77) for Ω. For these and other reasons, Ravndal [47] chose rather than (73)

$$G(m^*, q^2) = \exp\,[-K^{*2}/\Omega]\,\exp\,[1\,5\,q^2]\,(1 - q^2/4m^{*2})^{1-N},$$
$$K^* = (m^{*2} - m^2)/2m^*. \tag{79}$$

This insures a good fit to the pion form factor if we replace $\tilde{s}$ given by (76), with

$$\tilde{s}(m = m^*) = \tfrac{1}{2}, \tag{80}$$

which removes an embarassing zero in the π form factor at $q^2 = -4\,m^2_\pi$ Fortunately these difficulties with the elastic form factor will not cause us especial pain, as we shall only use (75) for off-diagonal matrix elements. Further, we will take them only at $t = 0$ and so avoid the ambiguities in the phenomenological q^2 dependence of (79)

In our numerical calculations, we take [6, 47] $\Omega = 1$ (GeV/c)^2.

References

[1] J.L. Rosner, review talks at Caltech and Argonne, UCRL-20655 (1971) and ANL/HEP-7208 (1972).
[2] F Gilman and N Samios, review talks at the 1972 Philadelphia Conf on experimental meson spectroscopy – AIP Conference Proceedings, No. 8
[3] G.C Fox, review talk at 1972 Philadelphia Conf. (ibid).
[4] D.W.G.S Leith, review talk at 16th Int. Conf on high energy physics, Batavia, 1972
[5] G.C Fox, π-exchange in ANL/HEP-7208, Vol II, p. 545.
[6] R P Feynman, M Kislinger and F Ravndal (hereafter FKR), Phys. Rev. D 3 (1971) 2706
[7] M Kislinger, Vector, tensor and pomeron-Regge couplings, Caltech preprint CALT-68-341 (1971)
[8] Particle Data Group, Phys Letters 39B (1972) 1.
[9] H. Harari, in Proc of the 14th Int. Conf on high energy Physics, Vienna, 1968 (CERN, Geneva, 1968)
[10] E W. Colglazier and J.L. Rosner, Nucl. Phys. B27 (1971) 349.
[11] E W Colglazier, Caltech thesis (1971).
[12] J.L. Rosner and E W. Colglazier, Phys Rev Letters 26 (1971) 933, M. Aguilar-Benitez et al., Phys Rev. Letters 25 (1970) 1635.
[13] J Mandula, J. Weyers and G. Zweig, Ann. Rev. Nucl. Sci 20 (1970) 289.
[14] G C. Fox, Cambridge thesis (1967).
[15] A D Martin and C Michael, Phys Letters 37B (1971) 513.
[16] G.C. Fox, in Phenomenology in particle physics, 1971, ed. C.B. Chiu, G C Fox and A.J G. Hey (Caltech, 1971).
[17] C Michael, CERN-TH-1480 preprint (1972), review talk at the 1972 Oxford Conf
[18] M Ross, F S Henyey and G.L. Kane, Nucl Phys 23B (1970) 269
[19] A V. Stirling et al , Phys. Rev. Letters 14 (1965) 763.
[20] P Sonderegger et al , Phys Letters 20 (1966) 75.
[21] Durham-Nijmegen-Paris-Torino Collaboration, Nucl Phys B22 (1970) 45
[22] P. Astbury et al , Phys. Letters 23 (1966) 396
[23] A. Bashian et al , Phys. Rev. D4 (1971) 2667.
[24] P. Kalbaci et al , Phys. Rev. Letters 27 (1971) 74.
[25] S.M. Pruss et al , Phys. Rev. Letters 23 (1969) 189.
[26] D.J Crenell et al., Two-body strange particle final states in π^-p interactions at 4 5 and 6 GeV/c, Brookhaven preprint (1972).
[27] L. Moscoso et al , Nucl. Phys. B36 (1972) 332.
[28] CERN-Munich Group, Analysis of the (s–p)-wave density matrix of the dipion system in the reaction $\pi^-p \to \pi^+\pi^-n$ at 17 GeV, preprint submitted to the 16th Int. Conf. on High energy physics Batavia, 1972.
[29] P Estabrooks and A.D Martin, Phys. Letters 41B (1972) 350
[30] R D Field et al., Study of vector-meson production with hypercharge exchange, Brookhaven preprint (1972)
[31] P Sonderegger in High-energy collisions (Gordon and Breach, 1969).
[32] G Goldhaber et al , Phys. Rev Letters 23 (1969) 1351, S. Hagopian et al., Phys Rev. Letters 25 (1970) 1050, B.N. Ratcliff et al., Phys. Letters 38B (1972) 345.
[33] A.S. Goldhaber, G.C. Fox and C Quigg, Phys Letters 30B (1969) 249.
[34] N Armenise et al , Nuovo Cimento 65A (1970) 637.
[35] I.J. Bloodworth et al , Nucl. Phys. B35 (1971) 79 and later erratum.
[36] M. Aguilar-Benitez et al., Study of non-strange mesons produced in K^-p interactions at 3.9 and 4.6 GeV/c, Brookhaven preprint BNL-16675 (1972)

[37] M. Abramovich et al , Nucl. Phys. B39 (1972) 189
[38] M Aguilar-Benitez et al , Phys. Rev Letters 28 (1972) 574.
[39] B Musgrave, private communication.
[40] J. Mott et al., Phys. Rev. 177 (1969) 1966.
[41] A.C. Ammann et al., Final states with three charged particles and a visible Λ from K^-d interactions at 4.5 GeV/c, Purdue preprint (1972).
[42] W A. Cooper et al., Nucl. Phys. B23 (1970) 605
[43] SABRE Collaboration, Nucl Phys B29 (1971) 557
[44] A G Clark and L. Lyons, The reactions $K^-p \to Y^0$ + vector meson at 3 15 and 3.3 GeV/c and the quark model, Oxford preprint (1971).
[45] J J. de Swart, Rev Mod Phys 35 (1963) 916.
[46] L A Copley, G Karl and E Obryk, Phys Letters 29B (1969) 117 and Nucl Phys B13 (1969 303
[47] F Ravndal, Phys Rev D4 (1971) 1466.
[48] L A Copley, G Karl and E Obryk, Phys Rev D4 (1971) 2844
[49] F E Close and F J Gilman, Phys. Letters 38B (1972) 541.
[50] C Michael and P V Ruuskanen, Phys. Letters 35B (1971) 65,
J L Rosner, Theoretical remarks on the A_2 meson, in Phenomenology in particle physics, 1971 (Caltech)
[51] U E Kruse, Partial wave analysis of A_2 production, preprint submitted to 16th Int Conf on high-energy physics, Batavia, 1972
[52] Yau-wu Tang, Measurements of the A_2^- and A_2^+ mass spectra, thesis (1971)
[53] A Peekna et al , Nucl Phys B27 (1971) 605
[54] BGLOR Collaboration, Phys Rev 152 (1966) 1148
[55] J Badier et al , 1964 Dubna Conf. Proc., p. 650
[56] ABCLV Collaboration, Nucl Phys B5 (1968) 606
[57] W Kropac et al , K^-d interactions at 5 5 GeV/c $\Sigma^{\mp}\pi^{\pm}\pi^-(\pi^0)$, $\Sigma^-K^+K^-$ and $K^-\pi^-p$ final states in which a hyperon is produced, preprint (1972)
[58] V E Barnes et al., Phys Rev Letters 15 (1965) 322
[59] D G Scotter et al , Nuovo Cimento 62 (1969) 1057
[60] G S Abrams et al , Phys. Rev Letters 18 (1967) 620.
[61] True reference unknown $K^-n \to h^0\Sigma^-$ data at 2 1 GeV/c quoted in CERN/HERA 70–6, Compilation of K^- induced reactions by E Flaminio et al
[62] ABBBHLM Collaboration, Phys Rev 138 (1965) B897
[63] SABRE Collaboration, Phys Letters 33B (1970) 631
[64] R E Berg, Study of the reactions $K^-n \to \pi^-\pi^-\pi^+\Sigma^0$, and $K^-n \to \pi^-\pi^-\pi^+\pi^0\Lambda$ at 4 91 GeV/c, Vanderbilt thesis (1971),
R E Berg et al , Nucl Phys B39 (1972) 509
[65] M Afzal et al , Properties of the B meson in 11 GeV/c $\pi^{\pm}p$ interactions, paper submitted to the 16th Int Conf on high-energy physics, Batavia, 1972.
[66] J H Campbell et al , Phys Rev Letters 22 (1969) 1204
[67] O I Dahl, L.M Hardy, R I Hess, J. Kirz and D H Miller, Phys Rev 163 (1967) 1377
[68] M Bardadin-Otwinowska et al , Phys Rev D4 (1971) 2711
[69] R Ammar et al , Phys Rev D2 (1970) 430
[70] C L Pols et al , Nucl Phys B25 (1970) 109
[71] N Armenise et al , Study of B^- resonance and $p\omega\pi$ channel in π^-p interactions at 9.1 GeV/c, paper submitted to 16th Int Conf on high-energy physics, Batavia, 1972
[72] D J Crenell et al , Phys Rev Letters 22 (1969) 1327
[73] R L Ott et al , Properties of the B(1235) meson produced in π^+p interactions at 7.1 GeV/c, abstract submitted to the 16th Int Conf on high-energy physics, Batavia, 1972
[74] F Ravndal, Phys Letters 37B (1971) 300

[75] M. Testa, Phys. Letters 42B (1972) 267
[76] M. Kislinger and K. Young, private communication
[77] ABCLV Collaboration, Nucl. Phys B36 (1972) 373.
[78] J A.J. Matthews et al, Phys. Rev. Letters 26 (1971) 400
[79] J A.J Matthews et al., Phys Rev D3 (1971) 2561.
[80] J A.J Matthews et al, Nucl Phys B32 (1971) 366
[81] J.A J. Matthews et al, Nucl. Phys B33 (1971) 1
[82] H H Bingham et al, Phys. Letters 41B (1972) 635.
[83] L.E Holloway et al., Phys Rev Letters 27 (1971) 1671
[84] S.U Chung et al., Phys. Rev 165 (1968) 1491
[85] A Barbaro-Galtieri et al., Phys. Rev. Letters 20 (1968) 349.
[86] W L. Yen et al., Phys Rev 188 (1969) 2011
[87] V E Barnes et al, Phys Rev Letters 23 (1969) 610.
[88] J. Ballam et al., Phys. Letters 31B (1970) 489
[89] J D Prentice et al, 4-Prong π^+p interactions at 5 5 GeV/c, preprint (1971)
[91] N.N. Biswas et al., Phys. Rev D2 (1970) 2529
[91] J A Gaidos et al, Phys Rev. D1 (1970) 3190
[92] J A Gaidos et al, Nucl Phys. B26 (1970) 225.
[93] A Dzierba et al., NAL proposals 54 and 110A
[94] J Ballam et al, Phys Rev Letters 24 (1970) 1364.
[95] Y Eisenberg et al, Phys Rev. Letters 23 (1969) 1322
[96] W. Podolsky, UCRL-20128, thesis (1971)
[97] R Carlitz and M. Kislinger, Phys Rev D2 (1970) 336.